THE PENNSYLVANIA STATE UNIVERSITY
SCHREYER HONORS COLLEGE

DEPARTMENT OF MECHANICAL ENGINEERING

DEVELOPING A FRAMEWORK FOR UNCERTAINTY QUANTIFICATION OF A CHEMICAL KINETIC PARAMETER IN MOCVDS

KARTIK KHOSA
FALL 2019

A thesis
submitted in partial fulfillment
of the requirements
for a baccalaureate degree
in Mechanical Engineering
with honors Mechanical Engineering

Reviewed and approved* by the following:

Yuan Xuan
Assistant Professor of Mechanical Engineering
Thesis Supervisor

Jacqueline O'Connor
Associate Professor of Mechanical Engineering
Honors Adviser

* Signatures are on file in the Schreyer Honors College.

ABSTRACT

Transitional metal dichalcogenides (TMDs) have been an increasingly explored research area due to their various applications in solar cells and quantum computing hardware. However, the key challenge has been finding the optimum way to manufacture TMDs. The two most popular TMDs are WSe_2 and $MoSe_2$. Both of these are produced by chemical vapor deposition. It has been difficult to maximize the yield of TMDs because the cost of experimentation is high, and the experiment takes longer to set up and perform. Therefore, to overcome these challenges, simulations were run to model the conditions and understand the impact of various parameters on the yield of the TMDs. But the accuracy of the chemical model is still not fully understood.

In this thesis, the impact of the uncertainty in one of the key chemical kinetic parameters, activation energy, is explored. This thesis focuses on the production of WSe_2 specifically. The chemical model was split into five different categories according to the reaction types. It was found there was no uncertainty in one set of reactions and so that set was not perturbed during the sampling process. The other four sets were perturbed individually so the effects of activation energy of different reactions could be understood. However, due to time constraints, only three sets were fully sampled and simulated. From the CO release set, it was found the most sensitive reactions were the initial release reactions 1, 2, and 4 that decompose $W(CO)_6$. For the H_2 gain set, all the sensitive reactions had a positive correlation. For the H_2 loss set, similar reactions were important but had negative sensitivity coefficients. MATLAB was used to create our own model to predict simulation results that ended up giving an underpredicted output. From an L_2 norm analysis, it was found that slowing down even one reaction negatively affected the yield.

TABLE OF CONTENTS

LIST OF FIGURES

LIST OF TABLES

ACKNOWLEDGEMENTS

Writing this thesis was a long journey, and in this journey, I met a lot of new people that helped me in a lot of ways. I would like to start by thanking Dr. Yuan Xuan for letting me work for him in the computational reacting flows laboratory in summer of 2018. His constant guidance both professionally and academically have been one of the essential foundations to my success here at Penn State. He has taught me to be a more patient and thoughtful person.

I would also like to thank all the people who work in the computational reaction flows laboratory, especially Suhaib Zafar and Yash Shah. They have helped me tremendously at various points during the research. It was wonderful to collaborate with them and learn from them how to use Linux, the details of the NGA software, and how to present research work.

Another person that has been a key to my success is Dr. Jacqueline O'Connor. She has been through several of my whining sessions and has taught me to always keep my chin up and be confident. She has helped me prepare for interviews, clean up my resume and land my first internship. I am very grateful for her wisdom and her support towards me.

Finally, I would like to thank my parents for investing in my future and sending me to Penn State. My parents believed in me and encouraged me to apply to the honors program in freshman year, and then again in Sophomore year even when I did not believe that I had in me to get in. I have had the best 3 years of my life at Penn State and made so many friends who are so vital to my support system.

Chapter 1

Literature Review

Applications of Transition Metal Dichalcogenides (TMDs)

As the human population increases to roughly 8.5 billion (UN World Population Prospects Report), humans need more resources to produce electricity to meet the demand (Tainter). However, humans cannot continue to feed on dirty fuels such coal, oil, and natural gas because they raise global temperatures of both air and water leading to many undesired risks (Doll et al.). It is imperative to find alternatives or improve renewable energy technology that is currently being used. US Energy Information Administration data shows that the role of renewable energy is increasing and will continue to increase in the future as shown in Figure 1.

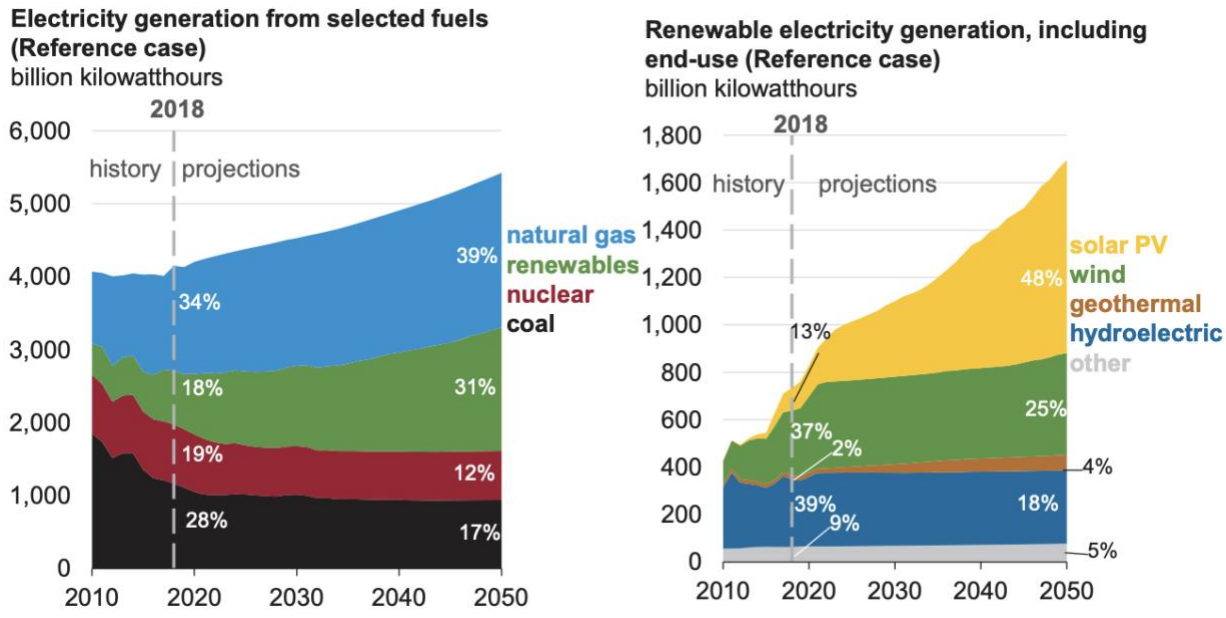

Figure 1 US Energy Information Administration electricity generation outlook

Solar energy is a viable option for many US households and commercial buildings to reduce CO_2 emissions (Alsema and Nieuwlaar). Currently, most solar cells use silicon wafers with graphene coating. Graphene is used as a transparent conducting electrode because of its low sheet resistance and high transparency (Khrapach et al. and Bae et al.). However, graphene has a low photoresponsivity and poor external quantum efficiency due to a zero-band gap and low light absorption coefficient (Nair et al. and Xia et al.). Graphene is a two-dimensional (2D) material because it is as thin as one carbon atom.

It is important to find alternate 2D materials that can replace graphene. Currently, many researchers are looking at 2D transitional metal dichalcogenides (TMDs) to replace graphene because of their large band gaps of 1-2eV and high carrier mobility. Transitional metal dichalcogenides are inorganic compounds that consist of one atom of a transition element and two atoms of Sulfur, Selenium or Tellurium. If a scalable technique of producing TMDs is found, not only can solar cell technology be improved immensely but also TMDs can revolutionize other parts of the electronic industries (Huang et al.). The next section of the literature review will consist of the development in the process of synthesizing transitional metal dichalcogenides.

Development in the synthesis procedures of Transition Metal Dichalcogenides

It is difficult to synthesize transitional metal dichalcogenides or predict how much will be produced (Eichfeld et al.). The process of synthesizing a specific TMD, tungsten diselenide (WSe_2), will now be discussed because WSe_2 will be the focus of this thesis. One of the first successful large area synthesis of WSe_2 was done using a metal organic chemical vapor

deposition system (MOCVDS) (Huang et al.). The team used tungsten oxide (WO_3) powder and placed it in a ceramic boat within a furnace. This boat was heated to 925 degrees Celsius. Selenium (Se) was heated upstream at 270 degrees Celsius. The Se vapors then reacted with the WO_3 vapors to give WSe_2 which then deposits at the sapphire substrates downstream. This process is followed by naturally cooing the substrate down from 750-850 degrees Celsius to room temperature as shown in Figure 2.

$$WO_3 + 3Se + H_2 \rightarrow WSe_2 + H_2O + SeO_2 \quad (1)$$

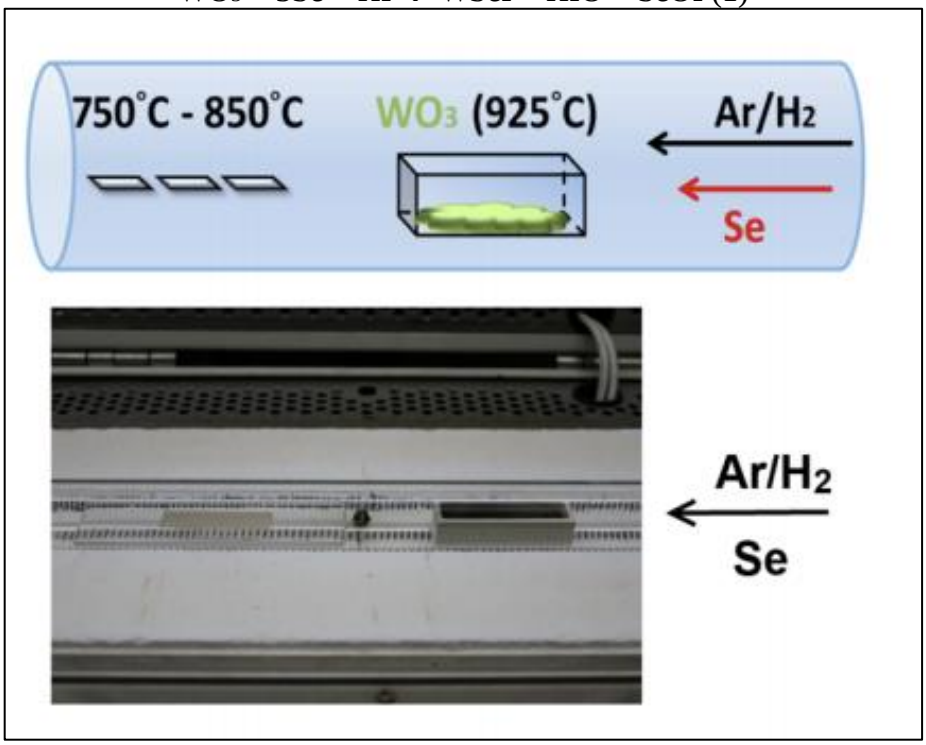

Figure 2 Schematic and photo of the setup for synthesis of WSe2 (Huang et al.)

The study found out that the use of H_2 is essential to enable the synthesis as H_2 is a strong reducer in the reaction. The first scalable and commercially viable synthesis process was introduced by the Pennsylvania State University. Researchers improved upon the MOCVD described earlier. They did so by changing the chemistry and the setup. Tungsten hexacarbonyl ($W(CO)_6$) and dimethyl selenium ($(CH_3)_2Se$) were used instead of tungsten trioxide (WO_3) and

Selenide (Se) so no powders were used unlike the experiments conducted by Huang et al. They used a similar approach of using hydrogen inside the metal organic chemical vapor deposition chamber. The new setup is shown in Figure 3.

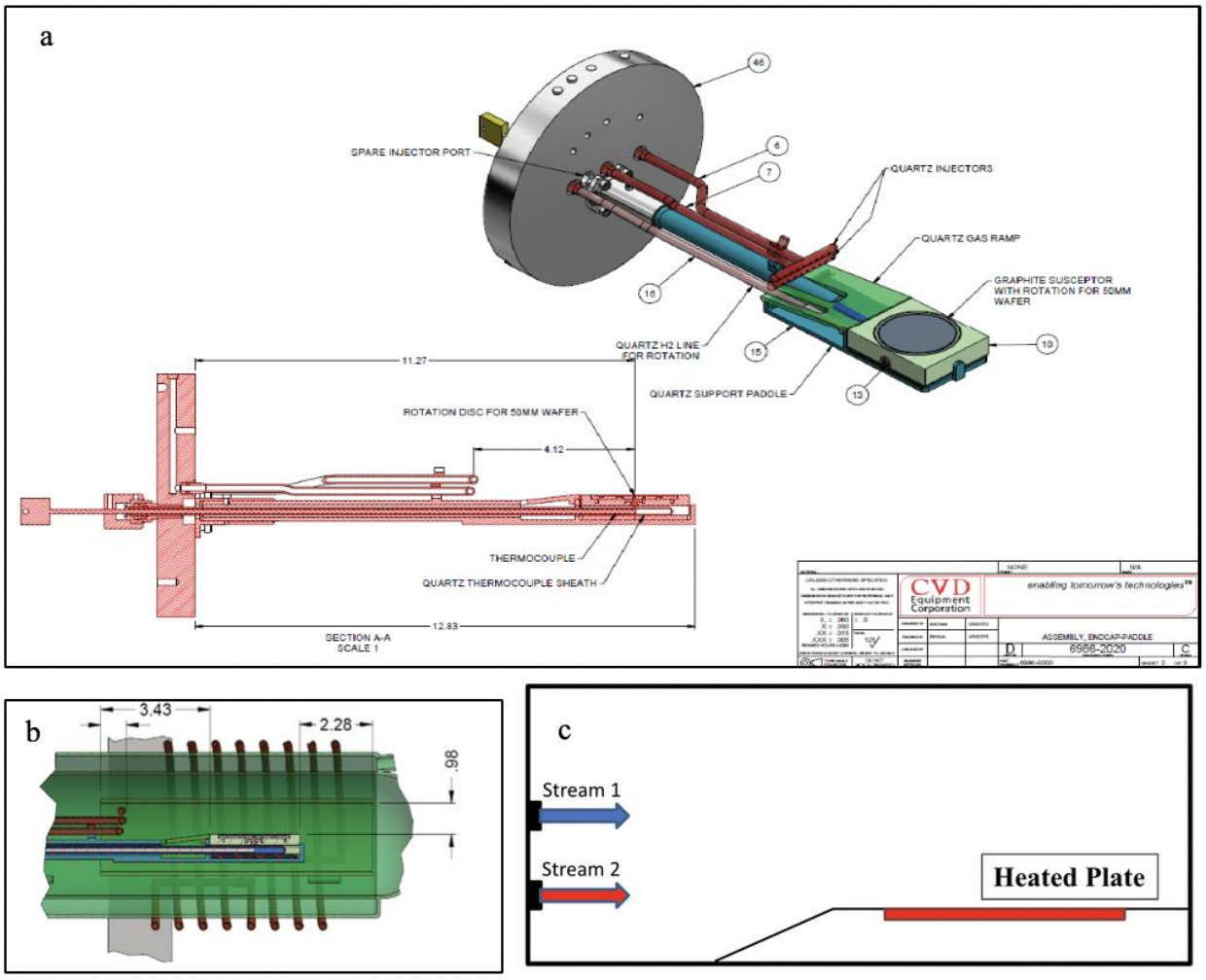

Figure 3 a) 3D Schematic of the MOCVD chamber from CVD Equipment Corporation, b) 2D Schematic of the MOCVD chamber from CVD Equipment Corporation, c) Simplified diagram of the chamber where stream 1 is dimethyl selenium ($(CH_3)_2Se$) and stream 2 is tungsten hexacarbonyl ($W(CO)_6$). (A. Jain, personal communication, May 13, 2018)

This process was the first time where the researchers were able to achieve monolayer control of large domain TMD structures (Eichfeld et al.). MOCVD chambers could now be used to control domain size, shape, and nucleation density of the transitional metal dichalcogenides

structures (Eichfeld et al.). Furthermore, synthesis via metal organic chemical vapor deposition can be highly scalable to meet industry requirements because MOCVD gives precise control over the gas-phase chemistry. This scalability was not possible with powder vaporization methods (Eichfeld et al.). However, Zhang et al.. later discovered that the process produced numerous defective layers of graphene instead of WSe_2 layers. This discovery meant that there was a problem with the chemistry. Zhang et al.. repeated the process and used hydrogen selenide (H_2Se) instead of dimethyl selenium ($(CH_3)_2Se$) as the starting reactant in stream 1 from Figure 3. The new results showed zero defective graphene layers meaning the extra carbon layers that were being formed, were due to the methyl radicals ($(CH_3)_2$) and not the from hexacarbonyl $(CO)_6$ radicals that were present in both the experiments.

Although metal organic chemical vapor deposition can be used to synthesis TMDs, information about the factors affecting the synthesis and production are still unknown. Eichfeld et al. conducted several parametric studies to learn more about the role of temperature, pressure, and flow rates in the synthesis of WSe_2 but further experiments need to be conducted to better understand the process. For example, there is little known about how the chemical kinetic parameters play a role in the synthesis of WSe_2. Nevertheless, conducting these experiments is really expensive in terms of the energy required to run the machinery and the cost of the equipment. Therefore, simulations must be conducted as a way of reducing cost and being able to predict results of experiments. The next section introduces a category of parameters whose effects are unknown on the synthesis of different species in the chemical vapor deposition chamber.

Methods of calculating chemical kinetic parameters

Chemical kinetic parameters are parameters that infer about the kinetic mechanisms for chemical conversion of reactions into products. These parameters essentially represent the rate of reaction and are influenced by temperature, pressure, concentration and other relevant factors. Chemical kinetic parameters can be calculated using ReaxFF (reactive force field) methods. ReaxFF is important in the field of molecular dynamics simulations because a lot of the information about chemical kinetic parameters is hard to determine experimentally. Furthermore, ReaxFF is more efficient than traditional force fields because ReaxFF eschews explicit bonds in favor of bond orders (Ostadhossein et al.). This means that a smooth transition can be achieved between nonbonded and bonded states while also retaining significant bond orders at a transition state (Ostadhossein et al.). Figure 4 shows the energy states for $W(CO)_6$ and the species formed when it decomposes. To calculate the activation energy for one reaction to take place, the difference between the two levels is measured and shown in Figure 4 using ReaxFF method and density functional theory (DFT).

Density functional theory is a method used to calculate the energy of interacting electrons. Electron interactions include two contributions: a classical (electrostatic) contribution and a quantum (exchange-correlation) contribution that depends on the electron density (Sholl & Steckel). This theory is the most popular theory in calculating chemical kinetic parameters. However, there are shortcoming related to this methodology. First, this method tends to underestimate the barriers of chemical reactions, the band gaps of materials, the energy of dissociating molecular ions, and charge transfer excitation energies (Cohen et al.). Furthermore, DFT also overestimates the binding energies of charge transfer complexes and the response to an

electric field in molecules and materials (Cohen et al.). In this thesis, activation energy used for simulations is determined using ReaxFF.

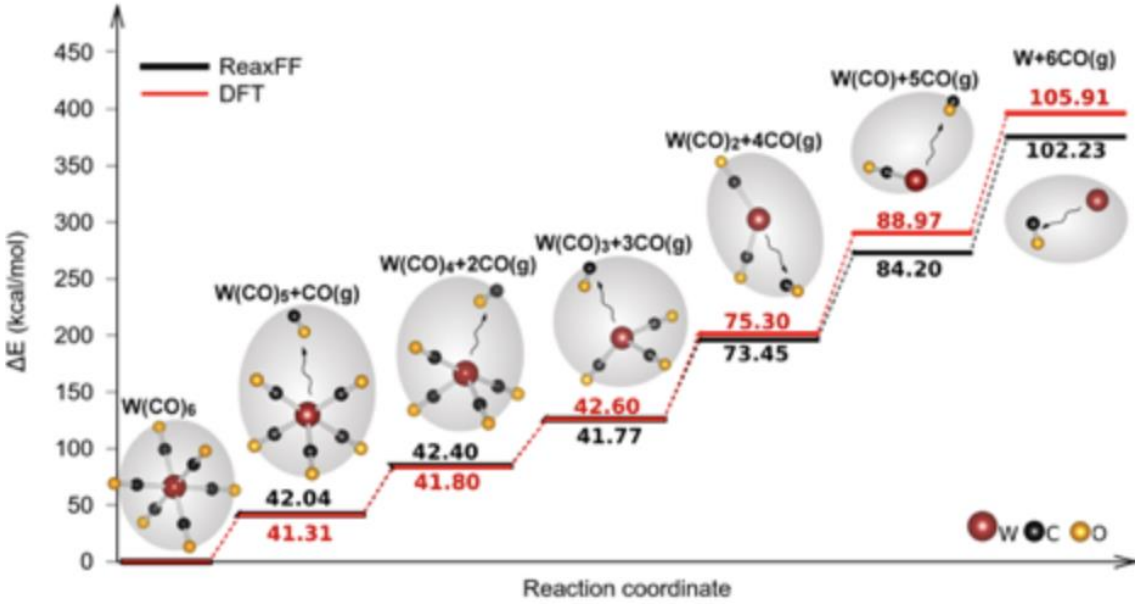

Figure 4 Energy state of different tungsten species during the decomposition of W(CO)6 (Y. Xuan, personal communication, February 13, 2019)

Because ReaxFF and DFT are not perfect models for estimating the exact chemical properties of materials, there is an uncertainty in the values obtained from the two methods. For example, ReaxFF values of bond dissociation energies, which help determine the activation energies, are within 5-10 kcal/mole in the study of Ostadhossein et al. This study was conducted for molybdenum disulfide (MoS_2), which is a close relative to tungsten diselenide (WSe_2). The next section will focus on what uncertainty propagation is and methods to quantify error propagation.

Quantification of chemical uncertainty effects

Uncertainty propagation occurs when uncertainty in the inputs is reflected as an uncertainty on the output. As discussed in the previous section, chemical kinetic parameters have uncertainties as they are calculated using computational tools and models. It is important that we must map the uncertainties of the values of chemical kinetic parameters so we can develop more accurate computer models for simulating MOCVD chambers. This will help us better predict experimental data while being cost efficient and safe.

One-way uncertainty propagation can be measured is through Monte Carlo simulations. This simulation methodology has been used as means to estimate answers to analytically intractable problems (Landau & Binder). For example, Döpking and Matera used Monte Carlo simulations to quantify the uncertainty propagation in a model of Carbon Monoxide (CO) oxidation on Ruthenium (IV) oxide (RuO_2). Because there is no theory that can fully explain this oxidation process, a model was developed and then tested using Monte Carlo simulations. Their model had 22 uncertain parameters. The rate constants and energy barriers (the 22 inputs) were calculated using DFT methods to develop the model, and Döpking and Matera considered these values to have a probability density functions due to the nature of DFT calculations. During the Monte Carlo simulations, 2_{18} or around 260,000 sample points were tested for these 22 inputs. It is important to note that this method was suitable in this case because the simulations were of 0_{th} dimension, meaning these simulations were computationally inexpensive.

Another way uncertainty propagation is quantified is through polynomial chaos expansion. Polynomial chaos is a method for expanding second-order randomness in terms of Hermite polynomials (Weiner). Second-order random processes are processes which have finite variances so this can be applied to most physical processes. Hermite polynomials are those that

are orthogonal, and continuous. There are two types of Hermite polynomials: probabilists and physicists. In a study from Zhang and Jiang, polynomial chaos expansion was used to examine the fuel variability effects on the combustion properties. The combustion reaction consisted of a total of 52 species and 325 reactions. The authors used 1,000,000 sample points for determining polynomial chaos coefficients. Furthermore, they calculated the Sobol indices, which is a sensitivity analysis technique used to determine the sensitivity of the outputs towards the inputs.

In addition, Latin hypercube sampling (LHS) can be conducted for uncertainty propagation. This method of sampling allows us to have an orthogonal sample, meaning no sample is repeated unlike in Monte Carlo simulations (McKay et al.). Latin hypercube sampling is used when the inputs of a model have a known uncertainty or a probability distribution function (McKay et al.). For instance, Fish and Burton used Latin hypercube sampling to quantify the effect of uncertainties in kinetic and photochemical data on model predictions of stratospheric ozone depletion. The model consisted of 41 chemical species, 3 unimolecular reactions, 53 bimolecular reactions, 10 termolecular reactions, 16 heterogeneous reactions and 27 photolysis pathways. There were a total of 139 variables in the model and the model was run 300 times. Regression techniques were later used for sensitivity analysis to see which variables had the highest impact on the ozone depletion. The 10 most important factors were highlighted, and it was decided that further study needs to be conducted for those factors. The next section will discuss the research objectives of this thesis in relation to the previous subsections.

Research objectives

A numerical model has been developed that predicts combustion reactions that take place in the metal organic chemical vapor deposition chamber. This thesis will focus on the synthesis of tungsten diselenide in the MOCVD chamber. There are 169 reactions that take place in the chamber and 59 species are formed before the final product tungsten diselenide is formed. For each of the 169 reactions, there are different chemical kinetic parameters that have been calculated from ReaxFF methods. However, this thesis will be focusing on quantifying the effects of uncertainty on one particular chemical kinetic parameter: activation energy. Activation energy is defined as the minimum quantity of energy which the reacting species (reactants) must possess in order to undergo a specific reaction measured in kilojoules/mole or kilocalories/mole. It has been determined that the error in the activation energy from the ReaxFF calculation is ±5 kcal/mole ($\pm 1\sigma$). To improve our numerical model of the MOCVD chamber, we must quantify this uncertainty so that the model can better predict the synthesis of the experiment.

Each simulation performed is complex because it is a function of time, and space (2 dimensions: x and y). The resources allocated to the project are limited and the time that the project needs to be completed within is brief. Therefore, traditional techniques of sampling and data analysis such as those mentioned earlier: Monte Carlo simulations, polynomial chaos expansions, and Latin hypercube sampling will not be adequate due to the fact that they are computationally expensive. Each reaction has one activation energy which leads to 169 activation energies and 169 inputs. It is not possible to run thousands of simulations and perturb these inputs individually. This strategy is effective only when the simulations are simple and take less time to perform. For example, Döpking and Matera as mentioned previously ran 260,000 simulations. Their total computational time was 1000 hours, meaning each simulation took

approximately 14 seconds. The MOCVD chamber model that is being improved has an estimated time period of 2 days to run to completion. Hence, a better sampling strategy must be used so fewer simulations are needed to be performed for saving time and resources. This study will be repeated for different models in the future that will involve different transition metal dichalcogenides. Therefore, this study will serve as a platform for the next researcher to further the knowledge of quantifying the uncertainty of chemical kinetic parameters in other TMDs.

Chapter 2

Methodology

In this work, there are over 100 input variables that are perturbed to determine their effects on the final output that is the yield on our hot graphite plate. This chapter will discuss the methods that have been used to run the simulations and get the results.

2.1 Solver

Simulations of reacting flow systems are particularly challenging. The chemistry of the reactions makes the system more complex. The computationally expensive nature of integration of the chemical source terms comes from four main challenges: 1) the non-linear Arrhenius form of the chemical reaction rate constants, 2) the typically large number of species involved, 3) the strong coupling between chemistry and transport processes (convection and diffusion) and 4) their very large magnitude (therefore smaller timescales).

2.1.1 Fluid Mechanics

The reacting mixture is assumed to contain a total of N species and their chemistry is assumed to be given by the chemical kinetics mechanisms involving K reactions, with forward and backward reactions counted separately. The chemically reacting flows of interest in the current study are of low Mach number (M_a), typically below 0.3. Under this condition, the acoustic waves can be ignored and the pressure field can be decomposed into a spatially-

invariant, but potentially time-dependent component, $P_0(t)$, and a fluctuating hydrodynamic pressure, p(x,t), with

$$\frac{p(x,t)}{P_0(t)} = O(M_a) \quad (2)$$

To reduce complexity of the numerical algorithm without losing generality, Soret and Dufour effects, body forces, and radiative heat transfer are ignored. In addition, the species molecular diffusion is assumed to be described by the Fickian law. Under these assumptions, the following are the conservation equations of mass, momentum, energy, and species density

$$\frac{\partial \rho}{\partial t} + \nabla \cdot (\rho \boldsymbol{u}) = 0 \quad (3)$$

$$\frac{\partial \rho \boldsymbol{u}}{\partial t} + \nabla \cdot (\rho \boldsymbol{u} \otimes \boldsymbol{u}) = -\nabla \mathrm{p} + \nabla \cdot \boldsymbol{\tau} \quad (4)$$

$$C_p \left[\frac{\partial \rho T}{\partial t} + \nabla \cdot (\rho \boldsymbol{u} T)\right] = \nabla \cdot \left(\rho C_p \alpha \nabla \mathrm{T}\right) + \sum_i C_{p,i} \rho \left(\frac{\alpha}{Le_i} \nabla Y_i + Y_i \boldsymbol{V_{c,i}}\right) \cdot \nabla T + \dot{\omega}_T \quad (5)$$

$$\frac{\partial \rho Y_i}{\partial t} + \nabla \cdot (\rho \boldsymbol{u} Y_i) = \nabla \cdot \left(\rho \frac{\alpha}{Le_i} \nabla Y_i\right) + \nabla \cdot \left(\rho Y_i \boldsymbol{V_{c,i}}\right) + \dot{\omega}_i \quad (6)$$

In the above equations, ρ is the density, **u** is the velocity vector, T denotes the temperature of the mixture, and Y_i is the mass fraction of species i. In the momentum equation (Eq. 4), $\boldsymbol{\tau}$ is the deviatoric stress tensor, defined as

$$\boldsymbol{\tau} = \mu[\nabla \boldsymbol{u} + (\nabla \boldsymbol{u})^T] - \frac{2}{3}\mu(\nabla \cdot \boldsymbol{u})\boldsymbol{I} \quad (7)$$

where **I** is the identity matrix and μ is the fluid viscosity. In the energy conservation equation (Eq. (5)), $\dot{\omega}_T$ includes heat source terms due to chemical reactions, α is the thermal diffusivity, and C_p is the specific heat at constant pressure of the mixture, given by

$$C_p = \sum_{i=1}^{N} Y_i C_{p,i} \quad (8)$$

where $C_{p,i}$ is the specific heat at constant pressure of species *i*. In the species conservation equations (Eq. (5)), $\dot{\omega}_i$ is the chemical source term of species *i* and Le_i is the Lewis number of species *i*, defined as

$$Le_i = \frac{\alpha}{D_i} \quad (9)$$

with D_i the mass diffusivity for species *i*. The correction velocity $\mathbf{V_{c,i}}$ in Eq. (6) accounts for the gradients in the mixture molecular weight as well as ensures zero net diffusion flux. It has the following expression

$$\boldsymbol{V}_{c,i} = \frac{\alpha}{Le_i}\frac{\nabla W}{W} - \alpha\left(\sum_{j=1}^{N}\frac{\nabla Y_i}{Le_j}\right) - \alpha\frac{\nabla W}{W}\left(\sum_{j=1}^{N}\frac{Y_j}{Le_j}\right) \quad (10)$$

where

$$W = \left(\sum_{j=1}^{N}\frac{Y_j}{W_j}\right)^{-1} \quad (11)$$

where represents the local mean molecular weight of the mixture, and W_j is the molecular weight of species *j*.

The above set of equations is contemplated by the equation of thermodynamic state

$$\rho = \frac{P_0 W}{\hat{R}T}$$

where P_0 is the thermodynamic pressure (see Eq. (2)) and $\hat{R}$ is the universal gas constant.

2.1.2 Chemical model

The overall rate of change of species *i*, $\dot{\omega}_i$ in Eq. (6) can be split into a production term, $\dot{\omega}_{i^+}$, and a consumption term, $\dot{\omega}_{i^-}$, as

$$\dot{\omega}_i = \dot{\omega}_i^{+} - \dot{\omega}_i^{-} \quad (13)$$

It is important to note that both the production term $\dot{\omega}_i^{+}$ and the consumption term $\dot{\omega}_i^{-}$ are positive.

The production rate of species *i*, $\dot{\omega}_i^{+}$, is given by the sum of the contributions from all the elementary chemical reactions leading to the formation of this species

$$\dot{\omega}_i^{+} = W_i \sum_{\substack{j=1 \\ v_{ji}>0}}^{r} \left[v_{ji} k_j \prod_{\substack{s=1 \\ v_{js}<0}}^{N} \left(\frac{\rho Y_s}{W_s} \right)^{-v_{js}} \right] \quad (14)$$

where *r* is the total number of chemical reactions and v_{js} is the stoichiometric coefficient of species *s* in reaction *j* (negative for reactants and positive for products). In the above expressions, the rate constant of reaction *j*, k_j, is given by the Arrhenius form, $k_j(T) = A_j T^{b_j} \exp\left(-\frac{T_{a,j}}{T}\right)$, where $T_{a,j}$ is the activation temperature of this reaction. Similarly, the consumption rate of species *i*, $\dot{\omega}_i^{-}$, is given by the sum of the contributions from all the elementary chemical reactions leading to the destruction of this species

$$\dot{\omega}_i^{-} = -W_i \sum_{\substack{j=1 \\ v_{ji}<0}}^{r} \left[v_{ji} k_j \prod_{\substack{s=1 \\ v_{js}<0}}^{N} \left(\frac{\rho Y_s}{W_s} \right)^{-v_{js}} \right]. \quad (15)$$

The local heat release rate is given by

$$\dot{\omega}_T = -\sum_{j=1}^{N} h_i \dot{\omega}_i \quad (16)$$

where

$$h_i = h_i^0 + \int_{T_0}^{T} C_{p,i} dT \quad (17)$$

is the specific enthalpy of species i, and h_i^0 denotes its value under standard reference conditions.

2.2 Chemical kinetic model

In the model's chemistry, there are five different sets of reactions. One set is a species losing CO molecule. Second set is a species losing a H_2 molecule and another is a species gaining H_2 molecule. These sets are similar because they are backward and forward reactions of each other. Final two set of reactions are also back and forward and involve species losing and gaining H_2Se molecule.

Table 1. Types and Number of Species and Reactions

Type of species	Number of reactions
Losing CO	41
Gaining H_2	32
Losing H_2	32
Gaining H_2Se	32
Losing H_2Se	32
Total Number of Species = 5	Total Number of Reactions = 169

Because there are five sets of reactions, it was determined that only one set should be perturbed. This means the activation energy of each of the reactions in one set will be perturbed together while all other activation energies of different reactions set should remain constant. The chemical kinetic model consists of two gas-phase precursors ($W(CO)_6$ and H_2Se) that are injected into the chemical vapor deposition chamber. These two break down through the 103 unimolecular reactions and 65 bimolecular reactions. One example of this is given in Figure 4 where the pathway of decomposition of $W(CO)_6$ is shown. In total, there are 59 gas species

involved. However, in real life the deposition is solid, and there is little understanding of how to correlate gaseous results from CFD into actual solid formed: for example, the lack of stick coefficient that can estimate the transfer of mass between solid and gas phase. This means that the cells that are just above the plate have to be used as an estimate for how much deposition is to be expected on the actual plate.

From Xuan et al., all the values of activation energies and Arrhenius coefficients for the different reactions are obtained. One thing to note is that this thesis is trying to quantify uncertain variables and the activation energy of all reactions in the gaining H_2Se set are 0 and certain. Thus, the 32 reactions in that set will remain unperturbed. The next section will discuss the method used for perturbing activation energies as it is the main focus of the thesis.

2.3 Latin hypercube sampling

In this thesis, saturated nearly orthogonal Latin hypercube sampling method was used. This method was devised by Hernandez. This technique focuses on minimizing the number of samples required for a large number of factors that are perturbed. The main way the method minimizes the number of samples is by focusing on keeping the correlation between each variable in all the samples low ($\rho <= 0.05$). What this means is that when data is analyzed, there is no confusion as to whether a particular factor is sensitive or important because it may have correlation to another factor.

From the study of Hernandez, two different sampling sets were used. Even though there are four sets that are being perturbed, only two are required because one set has 42 variables, and the other three have 32 variables. Therefore, the same sampling set can be used to create the

different sets of samples. The first sampling sets is given in Table 2. The code for generating the samples using Table 2 is given in Appendix A.1 and A.2. The sampling set used for CO release reactions is in Appendix B.

Table 2 Sampling set used to perturb Gaining H_2, Losing H_2 and Losing H_2Se reactions

	k1	k2	k3	k4	k5	k6	k7	k8	k9	k10	k11	k12	k13	k14	k15	k16	k17	k18	k19	k20	k21	k22	k23	k24	k25	k26	k27	k28	k29	k30	k31	k32
n1	14	23	5	18	10	26	4	7	31	32	10	8	1	1	3	12	20	28	18	17	27	24	24	12	3	24	24	23	26	8	17	32
n2	5	1	6	3	18	2	23	19	23	31	27	31	5	20	20	15	17	32	26	28	14	15	2	9	23	7	17	13	10	32	16	26
n3	26	6	8	17	32	5	2	13	29	14	32	14	21	18	23	32	29	13	21	15	26	6	22	25	5	9	29	7	30	13	22	2
n4	29	16	14	4	13	28	33	18	20	19	8	3	14	33	33	18	14	19	19	8	10	30	32	23	22	6	30	9	27	26	26	30
n5	13	29	3	6	14	30	20	32	18	3	21	33	28	19	7	13	22	11	24	2	11	5	7	14	2	8	6	27	28	15	23	27
n6	19	11	31	24	22	18	22	3	4	22	13	25	30	7	27	26	32	30	10	4	5	9	11	6	12	30	27	22	29	24	6	31
n7	2	10	28	30	6	17	13	16	22	2	15	15	11	21	16	21	24	22	29	12	13	1	31	4	25	14	15	4	2	5	33	24
n8	24	18	11	22	8	4	26	6	6	10	18	28	4	3	28	1	30	10	20	11	22	31	17	24	15	26	1	3	24	20	29	12
n9	30	26	7	23	11	11	24	28	17	7	31	13	9	13	24	16	5	33	6	1	19	20	6	11	20	18	32	15	4	1	4	15
n10	21	33	18	29	29	7	14	17	28	29	26	24	32	12	25	3	13	8	2	30	6	19	29	15	18	4	11	10	8	11	20	33
n11	15	14	21	31	30	33	1	33	11	12	6	18	10	25	29	14	33	26	12	27	21	29	1	27	10	13	19	16	7	19	24	19
n12	28	3	20	13	3	19	5	26	5	15	4	32	26	9	5	8	7	9	15	19	28	13	28	22	13	11	33	2	11	27	5	18
n13	18	24	10	21	7	21	8	4	19	33	7	29	29	32	9	28	6	27	7	9	18	16	3	26	32	20	9	5	25	10	30	7
n14	3	19	12	1	26	22	15	11	3	13	23	19	13	15	2	23	31	3	9	23	1	33	20	13	29	17	31	8	14	3	14	14
n15	23	30	33	16	4	29	17	20	25	28	22	27	2	10	30	33	8	1	30	26	4	11	8	17	6	22	21	12	15	18	15	8
n16	32	13	29	2	5	9	21	22	8	20	24	12	33	16	13	30	23	25	22	32	25	28	16	18	9	19	5	29	6	2	27	25
n17	4	21	25	8	33	1	19	27	27	5	3	30	17	8	19	25	1	23	17	14	16	25	27	29	16	32	22	25	16	17	28	16
n18	31	8	9	33	24	23	25	2	12	1	17	23	6	23	4	24	4	24	23	33	3	17	23	28	17	12	8	24	22	14	7	20
n19	16	12	30	27	12	3	31	15	30	24	1	17	18	22	6	4	27	7	25	10	12	21	5	20	19	1	28	31	20	6	13	5
n20	10	9	17	15	2	10	9	8	21	6	29	2	20	24	17	5	12	5	3	20	9	10	4	33	14	33	26	28	13	28	25	29
n21	25	17	4	20	17	8	3	23	26	17	9	6	23	17	15	31	25	6	28	3	8	27	19	16	27	25	2	19	3	31	1	22
n22	1	31	2	25	9	15	29	14	2	26	14	20	19	26	26	27	26	16	16	22	30	7	33	30	11	15	23	30	5	21	9	11
n23	9	27	26	11	16	25	32	21	32	9	16	4	25	4	11	17	28	29	14	29	23	8	13	32	26	16	10	1	23	22	2	13
n24	8	5	24	26	1	24	12	30	24	16	33	22	16	14	21	19	16	20	1	16	17	32	30	8	28	10	7	33	33	23	12	4
n25	11	28	15	14	15	13	6	9	16	4	11	16	27	31	32	7	9	14	33	31	29	22	12	1	24	23	20	17	32	9	3	17
n26	20	4	1	28	25	31	28	29	14	27	19	9	31	2	18	10	11	12	31	25	15	12	15	10	30	31	25	21	17	16	32	9
n27	12	20	22	32	23	6	30	31	7	23	20	5	8	28	1	29	10	4	8	18	31	18	10	5	8	21	14	6	31	25	18	28
n28	17	7	13	5	20	14	16	24	15	25	2	7	12	27	22	6	15	21	4	21	2	4	25	7	1	27	3	11	19	7	8	1
n29	27	22	32	10	31	20	11	25	9	30	30	21	3	29	12	2	21	18	27	6	24	3	26	31	33	29	12	26	21	12	10	21
n30	7	2	19	9	27	27	18	5	13	18	12	11	15	5	31	22	2	2	11	5	33	14	9	21	21	2	4	20	9	4	11	23
n31	22	15	23	12	28	32	27	1	33	11	25	26	22	30	8	11	18	15	13	13	32	23	21	3	7	28	16	18	1	29	19	6
n32	33	32	16	7	19	12	10	12	10	8	5	10	7	6	14	20	19	17	5	24	20	2	14	2	31	5	18	32	18	33	31	10
n33	6	25	27	19	21	16	7	10	1	21	28	1	24	11	10	9	3	31	32	7	7	26	18	19	4	3	13	14	12	30	21	3

Each column represents the variable (the activation energies of 32 reactions) and the row represents a single sample. The variables are split into 33 bins (a unique bin for every sample), which means that no two samples will have the same value for any given input variable. A bin is defined as an equally probably space on a normally distributed curve. It was decided that the middle point in each bin be chosen as a means to make the process easy. Note that the set below has 46 input variables but losing CO set only has 42 reactions. This means that we will be removing the last four columns as this sampling set can be used for all number of inputs below or

equal to 46. Because each bin is equally probable, analyzing the data is simpler and the technique used for data analysis will be discussed in the next section.

2.4 Stepwise Regression and Sensitivity Analysis

Stepwise regression is a regression method used to find correlation between multiple inputs to an output in an efficient way by adding or removing terms from the predicted model. In forward stepwise regression, terms are added to improve the accuracy of the model whereas in backward stepwise regression, terms are removed until model accuracy increases. All the simulation data must be first read in MATLAB and that is done through the code in Appendix A.3. Afterwards, forward stepwise regression will be used as it is the default in MATLAB as shown in code in Appendix A.4. During data analyses, since each of the variable has no correlation to another one, this method will be greatly useful for us to understand which reactions will have a significant impact on the yield of the final product. The parameters that are being set for the regression are 95% confidence level (so p-value is lower than 0.05) and the regression is linear.

Stepwise regression will not only point out which factors are most important but also give the coefficients for sensitivity analysis. These coefficients are the magnitude of slope in the regression that is obtained for each of the major reactions (see Eq 17) that is determined important from the p-values.

$$s_1 = \frac{d(Yield)}{d(Ea_1)} \quad (17)$$

As mentioned before, the data that is analyzed is in the gaseous layer just above the plate. This region is row/y-axis number 110 and column/x-axis numbers 131 to 268 in our matrix of the

chemical vapor deposition chamber. This means that regression is performed 138 times for each individual cell on the plate. In the next section, the use of Monte Carlo simulation as means for data analysis is discussed.

2.5 Monte Carlo Simulation

After finding each of important reactions and their sensitivity, the models created during the stepwise regression are run through a Monte Carlo simulation. In the Monte Carlo simulation, the variables in the sample set are perturbed 1000, 5000 and 10,000 times until error in finding the standard deviation is minimized as long as the simulation is not too demanding. In MATLAB as shown in Appendix A.5, randomly perturbed samples are generated with a standard deviation of 5 kcal/mole and then the model is used to predict the outcome (yield) thousands of times to predict mean and standard deviation. This data can explain the overall effect of perturbing the reaction set on the yield and variability of the yield.

2.6 Euclidean Distance

Euclidean distance is an important concept that is used to find distance to arbitrary points. This distance can be used to find the discrepancies between two lines as well and that is called L_2 norm. The equation for this is

$$L^2 = \sqrt[2]{\frac{\int_{x_i}^{x_f}\left(f(x)-g(x)\right)^2 dx}{\int_{x_i}^{x_f}\left(f(x)\right)^2 dx}} \qquad 18$$

Where *f(x)* is the original function and *g(x)* is the function whose discrepancy is being found relative to our original function. This method was used to find the simulation results that were heavily affected by the perturbations in the activation energies. The value for L_2 norm that was selected was 0.15. Any simulation outside this range can be considered to be heavily impacted by the perturbations in the activation energies. The next chapter contains the results and discussion for the four different simulations sets. The L_2 was calculated using the "trapz" integration function in MATLAB as shown at the end of Appendix A.3.

Chapter 3

Results

3.1 Baseline case overview

The baseline case was run before any perturbations were made to see how the mass fraction of WSe_3 varied in the chamber. It is known that the mass fraction of WSe_2 is very low compared to WSe_3 in the chamber. This phenomenon occurs because most of the WSe_2 forms when solid WSe_3 on the plate decomposes to the WSe_2. Since the model that is being used deals with only gaseous species, only WSe_3 is the species of interest and its distribution is shown in Figure 5. The key parameters that are constant throughout all the simulations are the temperature (1123K), pressure (26700 pascals), inlet concentrations and velocities of $W(CO)_6$ and H_2Se.

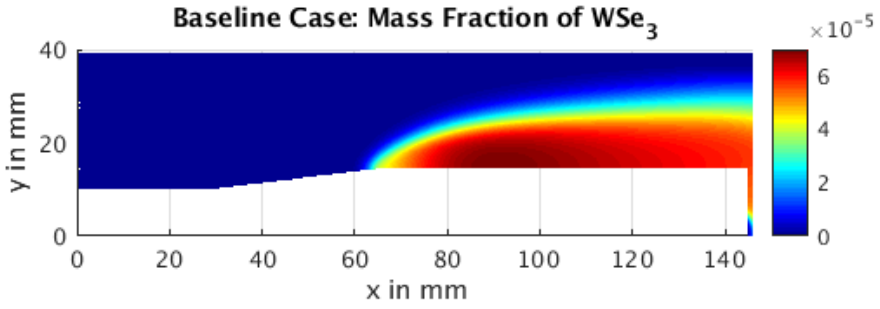

Figure 5 Spatial distribution of the mass fraction of WSe_3

The white region in Figure 5 represents the solid block that is present in the chamber and all the color is empty space occupied by the 59 species present in the chemical reactions that are

going on in the background. From Figure 5, it can be seen that WSe_3 starts to develop at the end of the ramp and its' mass fraction increases rapidly at that point and then the mass fraction reaches its peak point of highest mass fraction (dark red region) before it starts to drop off a little bit (light red/orange). This pattern is consistent with Figure 6, which shows the mass fraction of WSe_3 just above plate. This figure is important because the gaseous mass fraction on the plate relates directly to the solid deposition on the plate in real life.

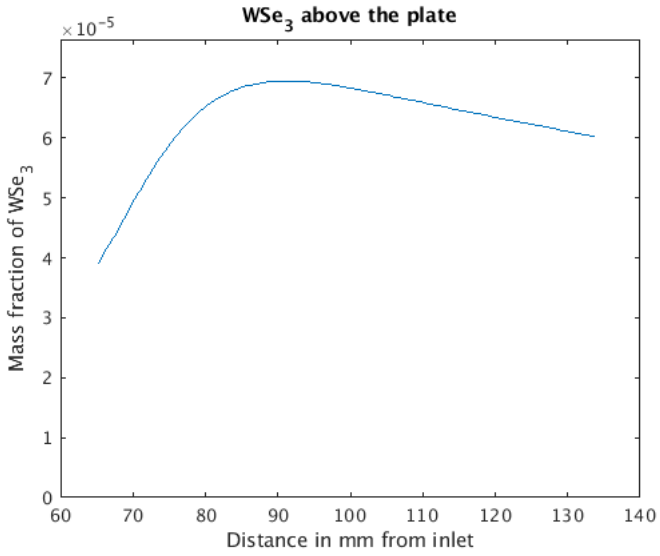

Figure 6 Mass fraction of WSe_3 at the point just above the heated graphite plate

3.2 Chemical kinetic uncertainty propagation for CO reactions

This set had 40 reactions and was perturbed 47 times. All simulation data from this set was run on the old chemical model where several reactions were missing, and the two missing CO reactions were not accounted for. Ideally there should be 42 reactions in our perturbations but because saturated nearly orthogonal Latin Hypercube sampling method was used, the post processing of the 40 reactions would not be that much different had there been 42 reactions.

Furthermore, due to the expensive nature of running the simulations, it was decided that rerunning the simulation would not be worth the effort and money.

In Figure 7, it can be seen that there is a huge variation in the results. Another thing to note is that the baseline used for comparison here is the baseline result from the old chemistry to keep consistency. Furthermore, the species of interest here is $W(H_2Se)_2Se_2$ because it gave the highest mass fraction in the old chemistry and it can decompose to WSe_2. Next, the most important reactions and their quantitative effect had to be determined. This was done using stepwise regression.

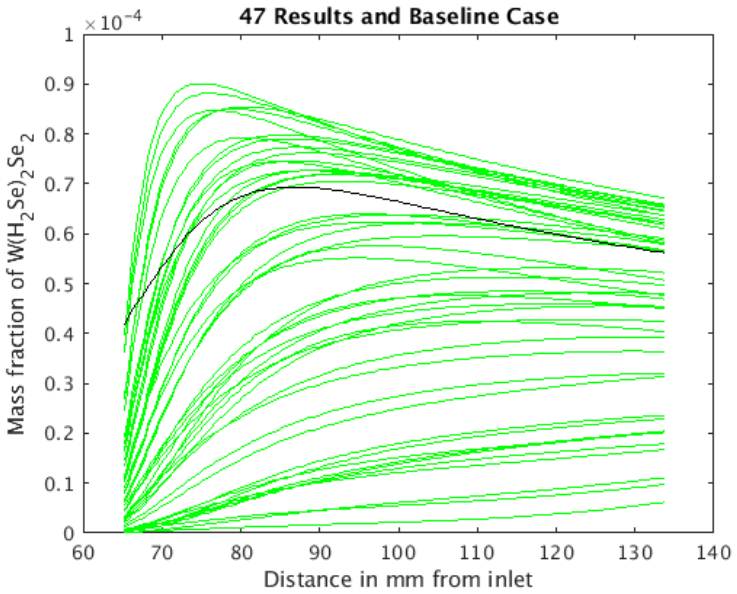

Figure 7 Mass Fraction of all the 47 simulations (green) and the baseline case (black) for CO loss set

Figure 8 shows the results obtained using forward stepwise regression. The left plot shows the reactions that were important at different spots above the plate. A colored dot means there is signifcant correlation between the activation energy of the reaction number and the mass fraction of the species of interest at that particular point above the plate. For example, reaction 15

is shown to be significant in the inception stage because the colored dots appear close to the start but disappear afterwards.

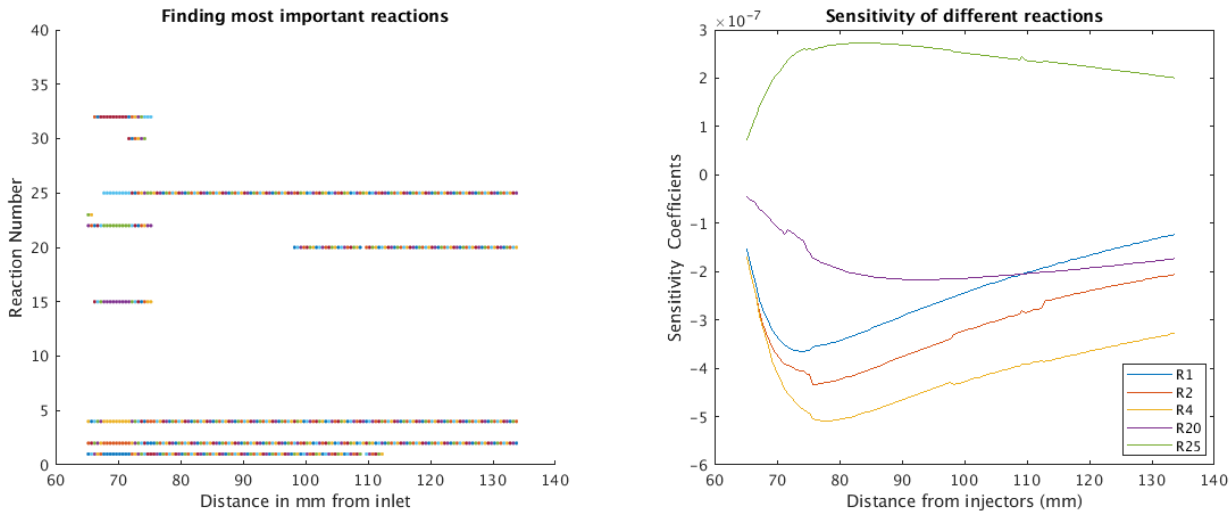

Figure 8 Results from stepwise regression of CO set

Five most important reactions were then used to calculate sensitivity coefficients. These five reactions were chosen based on their occurance (most number of dots). Reactions 1, 2, 4, and 20 show negative sensitivity whereas reaction 25 shows positive sensitivity. This means that when the activation energy in the models for positive sensitive reactions is increased, the mass fraction of $W(H_2Se)_2Se_2$ also increases and vice versa for negative sensitive reactions. Reaction 25 is somewhat strange as it would be expected that losing CO helps the reactants reach closer to the end species of WSe_3 so a negative sensitivity coefficient would be expected.

Additionally, a Monte Carlo simulation was performed after stepwise regression model had been made. In this simulation, the 40 samples were perturbed first 1000, then 5000 and then 10,000 times to find the mean and the standard deviation of the stepwise regression model. The results as shown in Figure 9 depict that the model underpredicts the baseline case when you

compare their means. The baseline values lie just outside the one standard deviation zone. Different number of points were chosen to make sure the error from randomization would be minimized. For future analysis, 5000 points are sufficient to give an accurate result of the simulation.

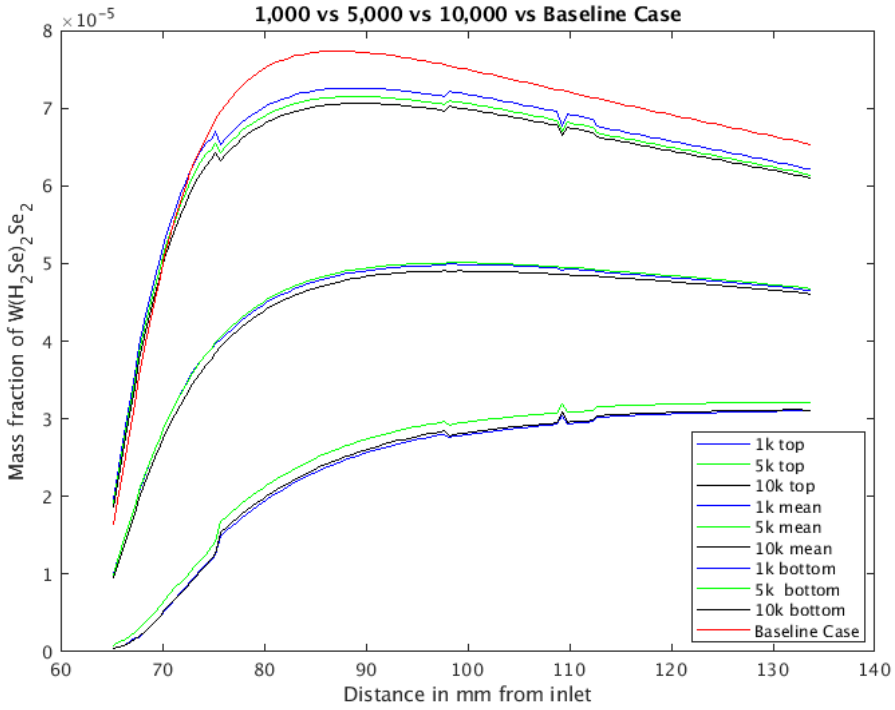

Figure 9 Result from Monte Carlo Simulation for CO reactions

Another implication of the underprediction means that even one reaction that is being slowed down can reduce the rate of production of all the other reactions. This makes sense as the first reaction to occur in the chamber is a CO release reaction. From the samples that we have generated, there is a 50 percent chance for each variable to be above the mean and 50 percent chance for them to be below the mean. Since we know the first reaction is important and half the time it is going to have an activation energy that is higher than its' mean, it is can be said that half of all reactions will be negatively impacted by that and thus many of the results are lower

than the baseline case. This will be true even if all of the later reactions were perturbed so that they would increase the yield because the first reaction is a limiting factor that bottle necks the chain of 169 reactions. To see how many bottle neck simulation results there were, an L_2 norm test was conducted and all the simulations were plotted as shown in Figure 10.

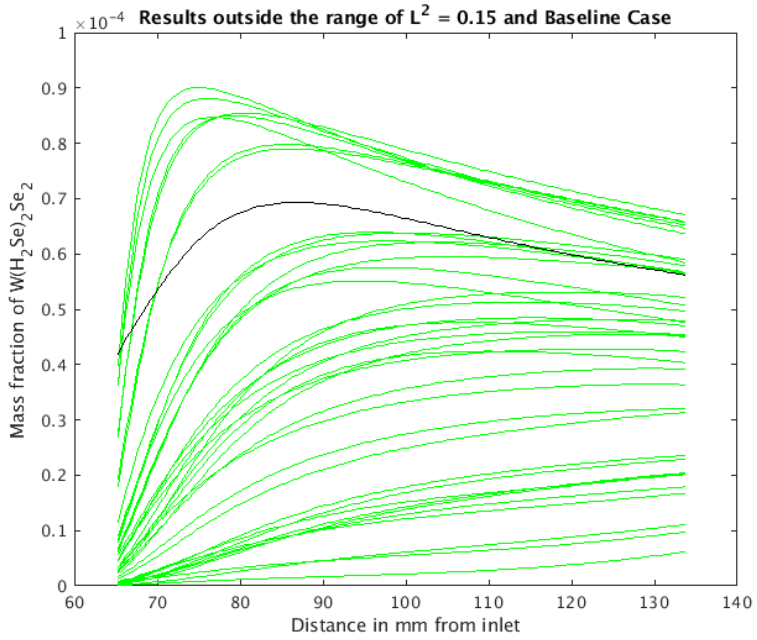

Figure 10 Results from filtering simulations via L_2 norm

In total, there were 37 reactions out of the 47 in total that were outside the range of 0.15 after L_2 norm was conducted. Out of the 37 simulations, 30 were under and 7 were over the baseline case. This once again explains the underestimation in our model.

3.3 Chemical kinetic uncertainty propagation for H_2 addition reactions

This set and all the next sets were simulated using the new chemistry. H_2 addition reactions took longer to reach steady state therefore, it took more than 50% time to simulate this set. This phenomenon could be explained due to the fact that H_2 reactions come after the CO

reactions. The decomposition of main input species $W(CO)_6$ begins with the species losing CO molecules and this can explain why CO sample set took less time to converge to steady state compared to H_2. Another reasoning for this could be the addition of the seven new reactions that were not present in the old chemistry. However, only one new H_2 addition reaction was added to the new chemistry so it is unlikely that will have any major impact.

Nevertheless, the results in Figure 11 show all the mass fractions that were obtained from the 33 different simulation results. Once again, there seems to be a small bias at the end of the plate that shows how these simulations are giving results that have lower yield than the baseline case.

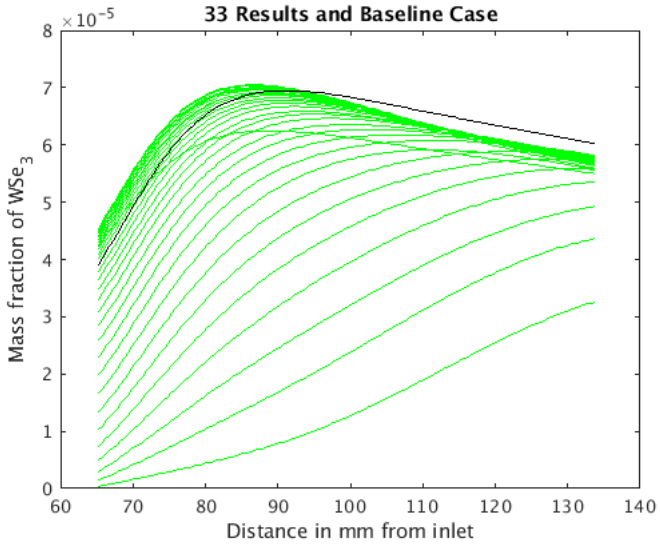

Figure 11 Mass Fraction of all the 33 simulations (green) and the baseline case (black) for H_2 addition set

Figure 12 depicts the most important reactions that influence the yield of the WSe_3. Reactions 8, 18, 21, 25, and 31 were chosen to be the top five and their sensitivity coefficients were also determined. It was surprising that all the reactions had positive sensitivity coefficients. This result means that when the activation energy is increased for these five reactions, the yield of WSe_3 increases. Furthermore, higher activation energy means there is higher difficultly in

achieving the products of the reaction, which means the species that are important for the yield to increase is on the reactants side of these reactions.

For example, reaction 21 seems to have the highest sensitivity. Reaction 21 is $W(CO)(HSe)_2Se_2 + H_2 \rightarrow W(CO)(H_2Se)_2Se_2$. This reaction is taking the W reactant away from the species of interest WSe_3, which means it is undesirable and therefore the positive sensitivity makes sense. Furthermore, this is true for all H_2 gain reactions and hence the sensitivity coefficients are all positive.

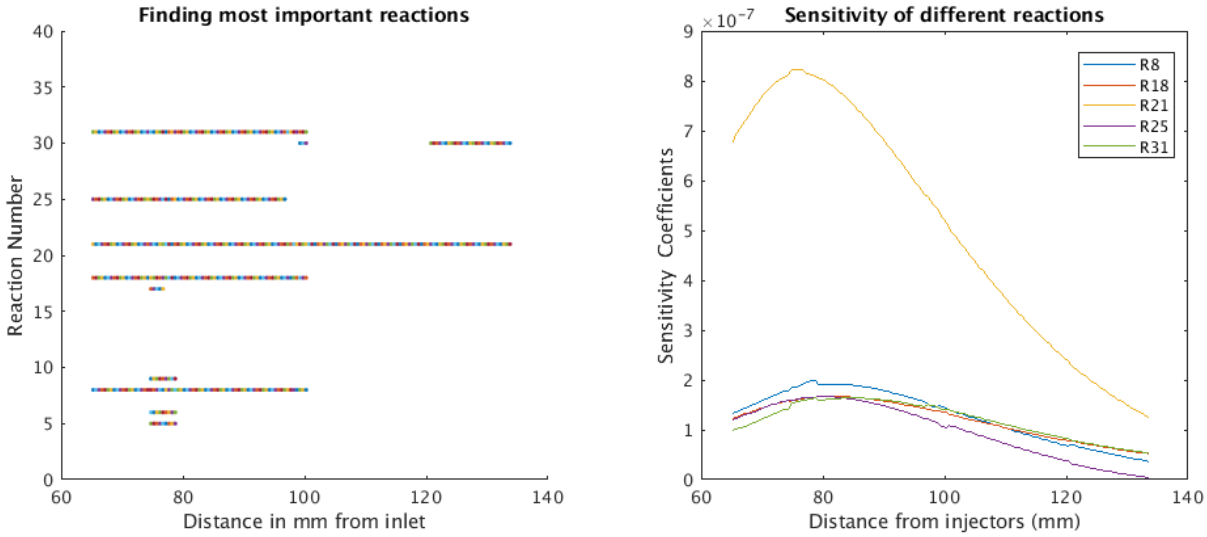

Figure 12 Results from stepwise regression of H_2 gain set

After performing a stepwise regression, the model was used to run simulations with 1000 and 5000 perturbed samples. This time 10,000 samples were not taken as the Monte Carlo simulation results were accurate enough by the time 5,000 samples had been taken. The results are shown in Figure 13. Compared to the CO reaction set, there is a smaller underprediction between the mean and the baseline case. Additionally, the baseline case mostly falls between the one standard deviation range.

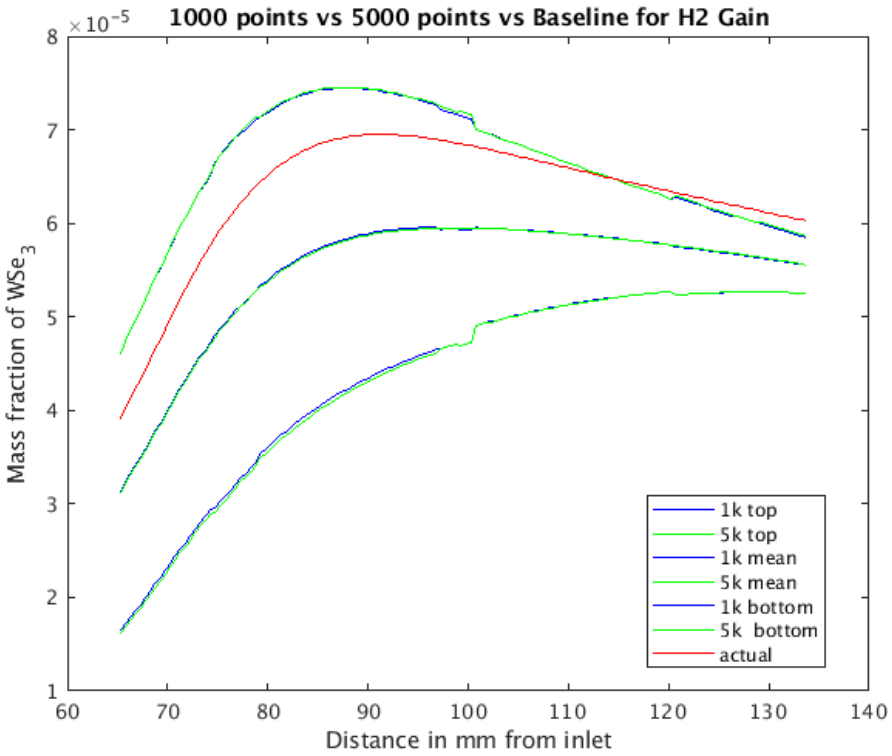

Figure 13 Result from Monte Carlo Simulation for H_2 gain reactions

The underprediction of the stepwise regression model is consistent with the fact that only one reaction is needed to be slowed for bottle necking the growth of WSe_3 as previously explained. Here the underprediction is less because CO reactions are at the start of the chain of all the other reactions whereas H_2 gain reactions come afterwards so have a smaller impact overall. To see how many results have been bottle necked, L_2 norm analysis was done between all the simulation results and the baseline case. The results are shown in Figure 14.

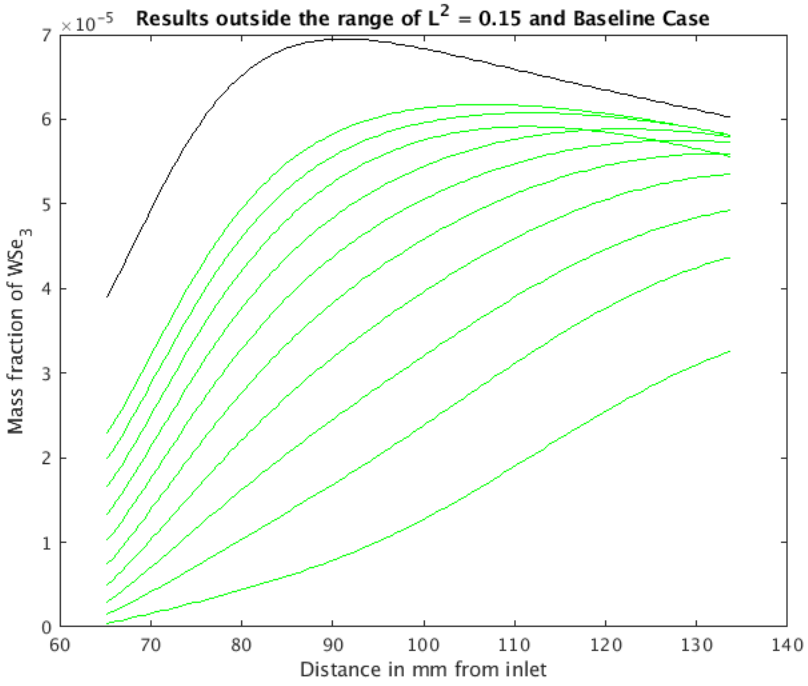

Figure 14 Results from filtering simulations via L_2 norm

Figure 14 shows there were 10 simulations that had limited the growth of WSe_3 and there were no simulations that over predicted by the criteria of $L_2 > 0.15$. Once again, there is evidence explaining why there is some underprediction.

3.4 Chemical kinetic uncertainty propagation for H_2 reduction reactions

One interesting thing about this set is the fact that it has the same reactions as the H_2 gain reactions, but they are reversed so it is expected the same reactions will be important. However, their sensitivity coefficients should be opposite of what they were for H_2 gain. To run the simulation to steady state, it took the same amount of time as H_2 gain reactions. The results of the 33 simulations is shown in Figure 15.

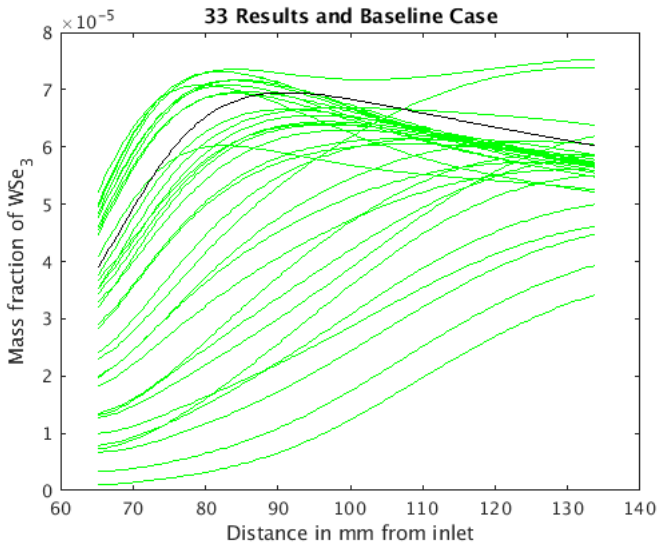

Figure 15 Mass Fraction of all the 33 simulations (green) and the baseline case (black) for H_2 reduction set

The results from the 33 simulations shows a variety of different mass fractions at different points in the plate just like the other two chemical sets did. Most of the simulation results have the same basic shape as the baseline case but there are many results that start very low and increase gradually. This is similar again to the other two chemical sets.

Figure 16 depicts the results from stepwise regression. Unlike the other chemical sets, there are fewer reactions that seem to matter: reaction 3, 18 and 21. It is strange that reaction 18 has a positive sensitivity coefficient. Just like all H_2 gain reactions have positive sensitivity, all the H_2 loss reactions should have negative sensitivity but only two out of the three main ones do. However, the magnitude of the sensitivity coefficient of reaction 18 is much smaller than those of reaction 3 and 21. Reaction 21 has the highest magnitude and therefore effect on the yield of WSe_3. This reaction is $W(CO)(H_2Se)_2Se_2 \rightarrow W(CO)(HSe)_2Se_2 + H_2$. It is the same as the reaction from H_2 gain set but in its' reverse form. It makes sense that these reactions are both important and their sensitivities are reversed for forwards and backwards reaction.

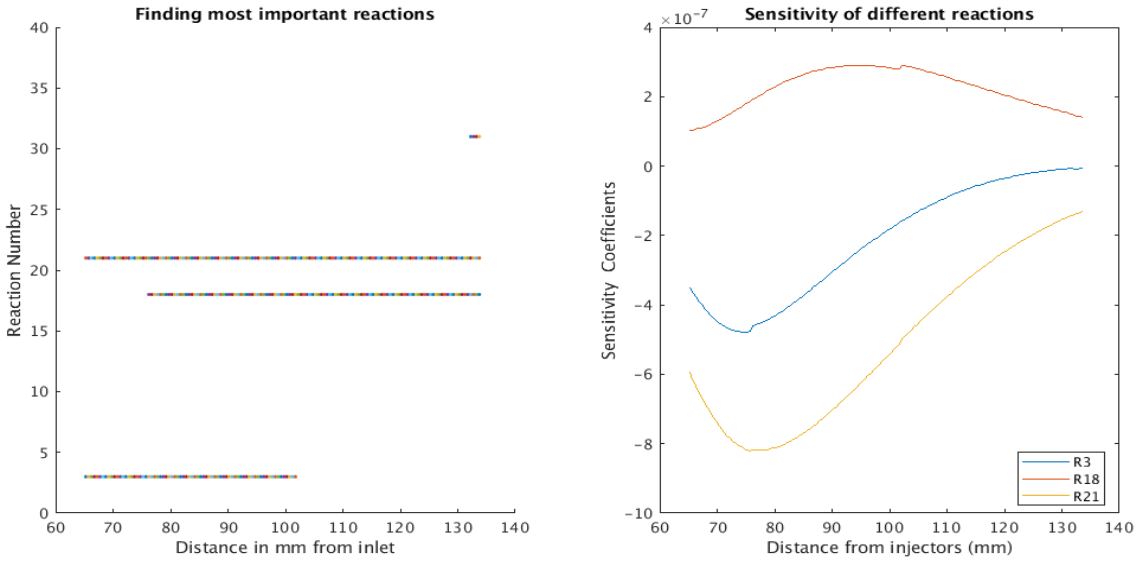

Figure 16 Results from stepwise regression of H_2 loss set

This set had some reactions that had negative activation energies in some of the samples. This abnormality in the samples could maybe explain the reverse behavior of reaction 18 as it had the opposite sign for sensitivity than was expected. Negative activation energy does not follow the law of Arrhenius where increase in temperature increases the rate of reaction. Instead, it is the opposite that the rate increases as the temperature decreases (Atkins and De Paula). The physical reason for this is molecules at higher temperatures shake themselves apart so quickly that they are not able to react the way they should and so the products form more slowly. Since the temperature in the chamber can reach 1123K, it is safe to say that the rate of reaction of that reaction is very low when the activation energy is negative. Therefore, at higher and positive activation energy, the rate of reaction is actually higher, and this leads to the positive sensitivity coefficient that can be seen in Figure 16 (right).

After the stepwise regression model was made, it was tested with Monte Carlo samples of 1000 and 5000 to give the results of mean and standard deviation shown in Figure 17. Compared to H_2 gain, the baseline case is not as close to the mean but still is in the +/- one standard

deviation range. There is some underprediction in model once again and the trend is not captured as well as the previous times.

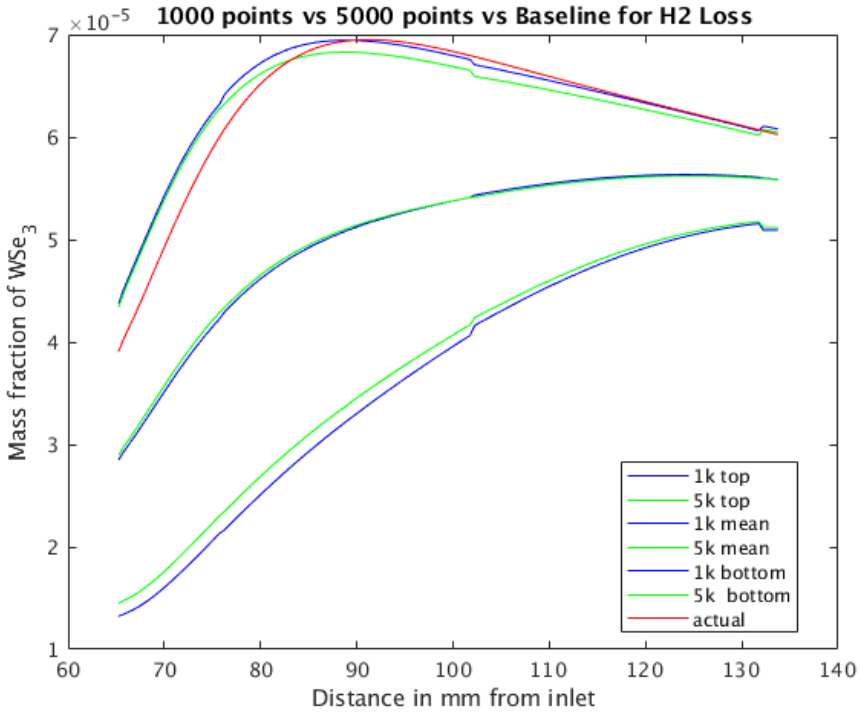

Figure 17 Result from Monte Carlo Simulation for H_2 loss reactions

To see why this was the case, another L_2 norm calculation was made for all the 33 simulations. It was found that there were 15 simulation results that were outside this range and all of them were in fact below the baseline case as can been seen in Figure 18. The shape of these 15 simulations is similar to that of the mean curve generated by the Monte Carlo simulation in Figure 17. The model is made based on the data from simulations so if most of the simulation data looks different to the baseline case, then the model will predict accordingly.

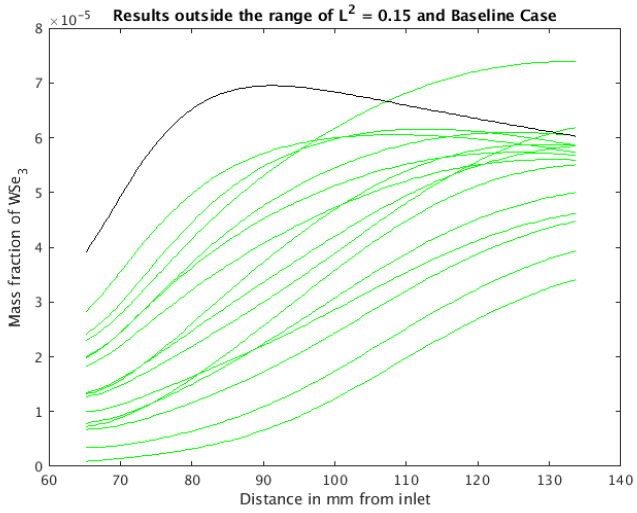

Figure 18 Results from filtering simulations via L_2 norm

Chapter 4

Conclusions and future work

This study examined the effects of changing activation energy of different reactions in the chemical model for a tungsten-selenium system. Using stepwise regression and sensitivity analysis, it was found that activation energy of most reactions have minimal effect on the yield of the $W(H_2Se)_2Se_2/WSe_3$ even though all reactions were perturbed equally.

For the set which involves CO release reactions, the most sensitive reactions were initial decomposition reactions of $W(CO)_6$ (which is one of the inputs). From the sensitivity analysis it was determined that as the activation energy increases for the initial decomposition reactions, a lower yield of the $W(H_2Se)_2Se_2$ will be deposited. This can be explained because if the initial reaction requires a lot of energy then it will need to get closer to the heated plate for a longer time. Therefore, all the other species that form also form later on the plate. Because there is less time for $W(H_2Se)_2Se_2$ to form, less of it is formed at the beginning and more of it is formed by the end. To improve our chemical model and reduce uncertainties, it would be beneficial to find more accurate values of these reactions because they can cause the values of yield to vary by almost a whole magnitude.

For the set which involves H_2 addition reactions, the most sensitive reactions were reactions 8, 18, 21, 25, and 31 and all had positive sensitivity. This was because all H_2 addition reactions make the reactants go back one step and away from the main goal of reaching WSe_3. Similarly, the set for H_2 reduction reactions, the most sensitive reactions (reactions 3 and 18) mostly had negative sensitivity because they all help the reactants get closer to reach WSe_3. However, there was one sensitive reaction (reaction 21) that had the positive sensitivity. This was due to the fact that some of the samples for that reaction were negative and this meant that

the reactions were actually slow because of the high temperature. Although it is unlikely that the activation energies may actually be negative, that activation energy of reaction 21 had smaller sensitivity coefficients (smaller impact) than the other two major reactions.

Additionally, the Monte Carlo analysis was useful because it showed the bias of underpredicting in our model and the bounds in which to expect the yield to be in real life. However, there are several improvements that could be made to improve the accuracy of the analysis as a whole. One improvement could be to add second order terms in the stepwise regression model to see if a reaction actually has a second order correlation instead of a linear correlation with the yield of $W(H_2Se)_2Se_2/WSe_3$. Another improvement can be to perform a further analysis by perturbing the factors (reactions) that were found the most important. This analysis would be the same as before but this time the variables will be very few therefore it would also be advised to use a less saturated sampling method than before.

Appendix A

MATLAB CODES

A.1 Example MATLAB code for generating a table of values for samples

```
clear
clc
%% creates a data set for H2 Gain
[numData2] = xlsread('32 variable LHS.xlsx');
[numData3 textData3 rawData3] = xlsread('Split 5 Categories After 7
Species.xlsx');
numData2 = numData2';
%%
[variables, samples] = size(numData2);
variables = variables - 1;
samples = samples - 1;
New_data = zeros(174,samples);
Start_of_category = 77; %% where each of the 5 categories start in excel
%%
for k = 1:samples
    New_data(1:173,k) = numData3(2:174,4);
end
%%
for j = 1:samples
    for i = 1:variables
        New_data((Start_of_category-2)+i,j) = norminv(((2*numData2(i+1,j+1)-
1)/(samples*2)),numData3(i+(Start_of_category-1),4),5*4.18);
    end
end
%% Check 1, checking for normality
for a = 1:variables
    [h(a),p(a)] = adtest(New_data(Start_of_category-2+a,:));
end
h
p
%%
Cell_converted_New_data = num2cell(New_data);
Final_table = rawData3;
Final_table((1:174),(5:4+samples)) = Cell_converted_New_data;
Final_table = cell2table(Final_table);
%%
writetable(Final_table,'Post Processed 5 Categories after 7
reactions.xlsx','WriteVariableNames',false)
```

A.2 Example MATLAB code for generating Linux friendly files from the tables

```
clear
clc

[numData, textData, rawData] = xlsread('Newest Chemical Model H2Se Loss
OCT.xlsx');
text = textData(:,2);
actual_numbers(1,:) = numData(:,3)';
isnancondition = isnan(numData);
mkdir Samples_H2Se_L
cd Samples_H2Se_L

for j = 1:33 %47 for CO and 33 for others
filename= sprintf('2DCC_%d.mech',j);
fid=fopen(filename,'w');

fprintf(fid,'Let al.lowed atoms be C, H, O, TU, SE.\n');
fprintf(fid,'Let temperature exponent be n_k.\n');
fprintf(fid,'Let order of reaction be n.\n');
fprintf(fid,'Let units for A be [ cm^(3(n-1)) / ( s * mole^(n-1) * K^n_k )
].\n');
fprintf(fid,'Let units for E be [ kJ / mole ].\n');

actual_numbers(2,:) = numData(:,j+4);

    for i = 1:length(numData)
        if numData(i) == 0
        fprintf(fid, '\n\n%s \n', text{i});
        elseif isnancondition(i) == 0
            fprintf(fid, '%d:', numData(i));
            fprintf(fid, ' %s', text{i});
            fprintf(fid, '              \t {A = %.2E n = 0.00 E = %.4f} \n',
actual_numbers(:,i));
        else
            fprintf(fid, '%s:', textData{i});
            fprintf(fid, ' %s', text{i});
            fprintf(fid, '              \t {A = %.2E n = 0.00 E = %.4f} \n',
actual_numbers(:,i));
        end
    end

    fclose(fid);
end

cd ..
```

A.3 Example MATLAB code for reading data and running L_2 norm from simulations

```
clear
```

```
%%
D = 33
P_TUSE3 = zeros(358,D);
P_sum_Yi = zeros(358,D);

[x,y,z,X,Y,xm,ym,zm,xper,yper,zper,icyl,~,~,~,mask,MASK] =
grid_reader('~/work/H2_GAIN/Sample1/config_sherlock');

%%

for counter = 1:33

filename= sprintf('~/work/H2_LOSS/Sample%d/data/data_1.000E+00',counter);

fid     = fopen(filename,'r');
dims    = fread(fid,4,'integer*4','ieee-le'); % read only the first 4
elements from the file

% Dimensions
nx      = dims(1);
ny      = dims(2);
nz      = dims(3);
nvar    = dims(4);

nsize   = nx*ny*nz;



% The following lines are necessary to move the file pointer to the correct
% location before you start reading in the variables
dt = fread(fid,1,'real*8','ieee-le'); % skippingC5H5(:,1)+A1XC6H6(:,1) +
A1C2H2(:,1) + A1CH3(:,1) + A2XC10H8(:,1) +A1C2H(:,1)/1.5 overdummy   =
fread(fid,nsize,'real*8','ieee-le');dt'
time = fread(fid,1,'real*8','ieee-le'); % skipping overdummy   =
fread(fid,nsize,'real*8','ieee-le');time'

varnames= [ ];

for var=1:nvar

    varnames = [varnames fread(fid,8,'*char','ieee-le') ]; % skipping over
the stored names
end

varnames;
MM(1)=0.3519024;
MM(2)=0.323892;
MM(3)=0.0280104;
MM(4)=0.2958816;
MM(5)=0.08097588;
MM(6)=0.40486788;
MM(7)=0.37685748;
```

```
MM(8)=0.2678712;
MM(9)=0.34884708;
MM(10)=0.45783336;
MM(11)=0.42982296;
MM(12)=0.45581748;
MM(13)=0.00201588;
MM(14)=0.42780708;
MM(15)=0.4538016;
MM(16)=0.4257912;
MM(17)=0.2398608;
MM(18)=0.32083668;
MM(19)=0.40181256;
MM(20)=0.51079884;
MM(21)=0.48278844;
MM(22)=0.39979668;
MM(23)=0.50878296;
MM(24)=0.48077256;
MM(25)=0.50676708;
MM(26)=0.47875668;
MM(27)=0.3977808;
MM(28)=0.2118504;
MM(29)=0.56376432;
MM(30)=0.56174844;
MM(31)=0.55973256;
MM(32)=0.55973256;
MM(33)=0.55771668;
MM(34)=0.29282628;
MM(35)=0.37380216;
MM(36)=0.45477804;
MM(37)=0.53575392;
MM(38)=0.37178628;
MM(39)=0.45276216;
MM(40)=0.3697704;
MM(41)=0.53373804;
MM(42)=0.45074628;
MM(43)=0.53172216;
MM(44)=0.52970628;
MM(45)=0.53172216;
MM(46)=0.26481588;
MM(47)=0.34579176;
MM(48)=0.42676764;
MM(49)=0.50774352;
MM(50)=0.34377588;
MM(51)=0.34176;
MM(52)=0.42475176;
MM(53)=0.42273588;
MM(54)=0.50572764;
MM(55)=0.50371176;
MM(56)=0.50169588;
MM(57)=0.50371176;
MM(58)=0.18384;
MM(59)=0.42072;
```

```
% There are usually 5 variables (or nvar number of variables) stored in the
data
% file: U, V, W, P, ZMIX. Each fread call makes the file pointer shift to the
end
% of the number of values read. Hence each subsequent fread call will start
after
% where the previous fread call stopped. Add on extra variables if necessary.

SUM_YI = zeros(nsize,1);

dummy   = fread(fid,nsize,'real*8','ieee-le'); U       =
reshape(dummy,nx,ny,nz);
dummy   = fread(fid,nsize,'real*8','ieee-le'); V       =
reshape(dummy,nx,ny,nz);
dummy   = fread(fid,nsize,'real*8','ieee-le'); W       =
reshape(dummy,nx,ny,nz);
dummy   = fread(fid,nsize,'real*8','ieee-le'); P       =
reshape(dummy,nx,ny,nz);
dummy   = fread(fid,nsize,'real*8','ieee-le'); RHO     =
reshape(dummy,nx,ny,nz);
dummy   = fread(fid,nsize,'real*8','ieee-le'); dRHO    =
reshape(dummy,nx,ny,nz);
dummy   = fread(fid,nsize,'real*8','ieee-le'); T6
=reshape(dummy,nx,ny,nz);SUM_YI = SUM_YI + dummy;
dummy   = fread(fid,nsize,'real*8','ieee-le'); T5
=reshape(dummy,nx,ny,nz);SUM_YI = SUM_YI + dummy;
dummy   = fread(fid,nsize,'real*8','ieee-le'); CO
=reshape(dummy,nx,ny,nz);SUM_YI = SUM_YI + dummy;
dummy   = fread(fid,nsize,'real*8','ieee-le'); T4
=reshape(dummy,nx,ny,nz);SUM_YI = SUM_YI + dummy;
dummy   = fread(fid,nsize,'real*8','ieee-le'); S2
=reshape(dummy,nx,ny,nz);SUM_YI = SUM_YI + dummy;
dummy   = fread(fid,nsize,'real*8','ieee-le'); T5S2
=reshape(dummy,nx,ny,nz);SUM_YI = SUM_YI + dummy;
dummy   = fread(fid,nsize,'real*8','ieee-le'); T4S2
=reshape(dummy,nx,ny,nz);SUM_YI = SUM_YI + dummy;
dummy   = fread(fid,nsize,'real*8','ieee-le'); T3
=reshape(dummy,nx,ny,nz);SUM_YI = SUM_YI + dummy;
dummy   = fread(fid,nsize,'real*8','ieee-le'); T3S2
=reshape(dummy,nx,ny,nz);SUM_YI = SUM_YI + dummy;
dummy   = fread(fid,nsize,'real*8','ieee-le'); T4GS2G2
=reshape(dummy,nx,ny,nz);SUM_YI = SUM_YI + dummy;
dummy   = fread(fid,nsize,'real*8','ieee-le'); T3GS2G2
=reshape(dummy,nx,ny,nz);SUM_YI = SUM_YI + dummy;
dummy   = fread(fid,nsize,'real*8','ieee-le'); T4GS1G2
=reshape(dummy,nx,ny,nz);SUM_YI = SUM_YI + dummy;
dummy   = fread(fid,nsize,'real*8','ieee-le'); H2
=reshape(dummy,nx,ny,nz);SUM_YI = SUM_YI + dummy;
dummy   = fread(fid,nsize,'real*8','ieee-le'); T3GS1G2
=reshape(dummy,nx,ny,nz);SUM_YI = SUM_YI + dummy;
dummy   = fread(fid,nsize,'real*8','ieee-le'); T4GSEG2
=reshape(dummy,nx,ny,nz);SUM_YI = SUM_YI + dummy;
dummy   = fread(fid,nsize,'real*8','ieee-le'); T3SE2
=reshape(dummy,nx,ny,nz);SUM_YI = SUM_YI + dummy;
```

```
dummy   = fread(fid,nsize,'real*8','ieee-le'); T2
=reshape(dummy,nx,ny,nz);SUM_YI = SUM_YI + dummy;
dummy   = fread(fid,nsize,'real*8','ieee-le'); T2S2
=reshape(dummy,nx,ny,nz);SUM_YI = SUM_YI + dummy;
dummy   = fread(fid,nsize,'real*8','ieee-le'); T2GS2G2
=reshape(dummy,nx,ny,nz);SUM_YI = SUM_YI + dummy;
dummy   = fread(fid,nsize,'real*8','ieee-le'); T3GS2G3
=reshape(dummy,nx,ny,nz);SUM_YI = SUM_YI + dummy;
dummy   = fread(fid,nsize,'real*8','ieee-le'); T2GS2G3
=reshape(dummy,nx,ny,nz);SUM_YI = SUM_YI + dummy;
dummy   = fread(fid,nsize,'real*8','ieee-le'); T2GS1G2
=reshape(dummy,nx,ny,nz);SUM_YI = SUM_YI + dummy;
dummy   = fread(fid,nsize,'real*8','ieee-le'); T3S2S12
=reshape(dummy,nx,ny,nz);SUM_YI = SUM_YI + dummy;
dummy   = fread(fid,nsize,'real*8','ieee-le'); T2S2S12
=reshape(dummy,nx,ny,nz);SUM_YI = SUM_YI + dummy;
dummy   = fread(fid,nsize,'real*8','ieee-le'); T3S2SE2
=reshape(dummy,nx,ny,nz);SUM_YI = SUM_YI + dummy;
dummy   = fread(fid,nsize,'real*8','ieee-le'); T2S2SE2
=reshape(dummy,nx,ny,nz);SUM_YI = SUM_YI + dummy;
dummy   = fread(fid,nsize,'real*8','ieee-le'); T2SE2
=reshape(dummy,nx,ny,nz);SUM_YI = SUM_YI + dummy;
dummy   = fread(fid,nsize,'real*8','ieee-le'); T1
=reshape(dummy,nx,ny,nz);SUM_YI = SUM_YI + dummy;
dummy   = fread(fid,nsize,'real*8','ieee-le'); T2GS2G4
=reshape(dummy,nx,ny,nz);SUM_YI = SUM_YI + dummy;
dummy   = fread(fid,nsize,'real*8','ieee-le'); T2S22S12
=reshape(dummy,nx,ny,nz);SUM_YI = SUM_YI + dummy;
dummy   = fread(fid,nsize,'real*8','ieee-le'); T2S22SE2
=reshape(dummy,nx,ny,nz);SUM_YI = SUM_YI + dummy;
dummy   = fread(fid,nsize,'real*8','ieee-le'); T2GS1G4
=reshape(dummy,nx,ny,nz);SUM_YI = SUM_YI + dummy;
dummy   = fread(fid,nsize,'real*8','ieee-le'); T2S12SE2
=reshape(dummy,nx,ny,nz);SUM_YI = SUM_YI + dummy;
dummy   = fread(fid,nsize,'real*8','ieee-le'); T1S2
=reshape(dummy,nx,ny,nz);SUM_YI = SUM_YI + dummy;
dummy   = fread(fid,nsize,'real*8','ieee-le'); T1GS2G2
=reshape(dummy,nx,ny,nz);SUM_YI = SUM_YI + dummy;
dummy   = fread(fid,nsize,'real*8','ieee-le'); T1GS2G3
=reshape(dummy,nx,ny,nz);SUM_YI = SUM_YI + dummy;
dummy   = fread(fid,nsize,'real*8','ieee-le'); T1GS2G4
=reshape(dummy,nx,ny,nz);SUM_YI = SUM_YI + dummy;
dummy   = fread(fid,nsize,'real*8','ieee-le'); T1GS1G2
=reshape(dummy,nx,ny,nz);SUM_YI = SUM_YI + dummy;
dummy   = fread(fid,nsize,'real*8','ieee-le'); T1S2S12
=reshape(dummy,nx,ny,nz);SUM_YI = SUM_YI + dummy;
dummy   = fread(fid,nsize,'real*8','ieee-le'); T1SE2
=reshape(dummy,nx,ny,nz);SUM_YI = SUM_YI + dummy;
dummy   = fread(fid,nsize,'real*8','ieee-le'); T1S22S12
=reshape(dummy,nx,ny,nz);SUM_YI = SUM_YI + dummy;
dummy   = fread(fid,nsize,'real*8','ieee-le'); T1S2SE2
=reshape(dummy,nx,ny,nz);SUM_YI = SUM_YI + dummy;
dummy   = fread(fid,nsize,'real*8','ieee-le'); T1GS1G4
=reshape(dummy,nx,ny,nz);SUM_YI = SUM_YI + dummy;
```

```
dummy   = fread(fid,nsize,'real*8','ieee-le'); T1S12SE2
=reshape(dummy,nx,ny,nz);SUM_YI = SUM_YI + dummy;
dummy   = fread(fid,nsize,'real*8','ieee-le'); T1S22SE2
=reshape(dummy,nx,ny,nz);SUM_YI = SUM_YI + dummy;
dummy   = fread(fid,nsize,'real*8','ieee-le'); TUS2
=reshape(dummy,nx,ny,nz);SUM_YI = SUM_YI + dummy;
dummy   = fread(fid,nsize,'real*8','ieee-le'); TUGS2G2
=reshape(dummy,nx,ny,nz);SUM_YI = SUM_YI + dummy;
dummy   = fread(fid,nsize,'real*8','ieee-le'); TUGS2G3
=reshape(dummy,nx,ny,nz);SUM_YI = SUM_YI + dummy;
dummy   = fread(fid,nsize,'real*8','ieee-le'); TUGS2G4
=reshape(dummy,nx,ny,nz);SUM_YI = SUM_YI + dummy;
dummy   = fread(fid,nsize,'real*8','ieee-le'); TUGS1G2
=reshape(dummy,nx,ny,nz);SUM_YI = SUM_YI + dummy;
dummy   = fread(fid,nsize,'real*8','ieee-le'); TUSE2
=reshape(dummy,nx,ny,nz);SUM_YI = SUM_YI + dummy;
dummy   = fread(fid,nsize,'real*8','ieee-le'); TUS2S12
=reshape(dummy,nx,ny,nz);SUM_YI = SUM_YI + dummy;
dummy   = fread(fid,nsize,'real*8','ieee-le'); TUS2SE2
=reshape(dummy,nx,ny,nz);SUM_YI = SUM_YI + dummy;
dummy   = fread(fid,nsize,'real*8','ieee-le'); TUS22S12
=reshape(dummy,nx,ny,nz);SUM_YI = SUM_YI + dummy;
dummy   = fread(fid,nsize,'real*8','ieee-le'); TUS22SE2
=reshape(dummy,nx,ny,nz);SUM_YI = SUM_YI + dummy;
dummy   = fread(fid,nsize,'real*8','ieee-le'); TUS12SE2
=reshape(dummy,nx,ny,nz);
dummy   = fread(fid,nsize,'real*8','ieee-le'); TUGS1G4
=reshape(dummy,nx,ny,nz);
dummy   = fread(fid,nsize,'real*8','ieee-le'); TU
=reshape(dummy,nx,ny,nz);SUM_YI = SUM_YI + dummy;
dummy   = fread(fid,nsize,'real*8','ieee-le'); TUSE3
=reshape(dummy,nx,ny,nz);
dummy   = fread(fid,nsize,'real*8','ieee-le'); T       =
reshape(dummy,nx,ny,nz);

sum_Yi = reshape(SUM_YI,nx,ny,nz);
a = 1.1;
for i = 1:nx
    for j = 1:ny
        if (MASK(i,j)<1)

            a  = min(sum_Yi(i,j),a);
        end
    end
end

a;

for i=1:nx
    for j=1:ny
        if(MASK(i,j)==1)
            H2(i,j)=0.0;
            sum_Yi(i,j)=0.0;
%             RHO(i,j)=NaN;
```

```
        end
    end
end

total_sum = T6+T5+CO+T4+S2+T5S2+T4S2+T3+T3S2+T4GS2G2+T3GS2G2+T4GS1G2+H2 ...
+T3GS1G2+T4GSEG2+T3SE2+T2+T2S2+T2GS2G2+T3GS2G3+T2GS2G3+T2GS1G2+T3S2S12 ...
+T2S2S12+T3S2SE2+T2S2SE2+T2SE2+T1+T2GS2G4+T2S22S12+T2S22SE2+T2GS1G4+T2S12SE2
...
+T1S2+T1GS2G2+T1GS2G3+T1GS2G4+T1GS1G2+T1S2S12+T1SE2+T1S22S12+T1S2SE2+T1GS1G4+
T1S12SE2 ...
+T1S22SE2+TUS2+TUGS2G2+TUGS2G3+TUGS2G4+TUGS1G2+TUSE2+TUS2S12+TUS2SE2+TUS22S12
+TUS22SE2+TUS12SE2 ...
+TUGS1G4+TU+TUSE3;

%concentration_new;
P_TUSE3(:,counter) = TUSE3(:,110);
%P_sum_Yi(:,counter) = sum_Yi(:,110)
counter

fclose(fid)

end

%% L2 norm
L2 = zeros(33,1);
for i = 1:33
L2_num = trapz(xm(131:268),(P_TUSE3_baseline(131:268)-
P_TUSE3(131:268,i)).*(P_TUSE3_baseline(131:268)-P_TUSE3(131:268,i)));
L2_den =
trapz(xm(131:268),(P_TUSE3_baseline(131:268)).*(P_TUSE3_baseline(131:268)));
L2(i) = sqrt(L2_num/L2_den);
end
L2_f = zeros(33,1);
for i = 1:33
    if L2(i) > 0.15
        L2_f(i) = i;
    else
        L2_f(i) = 0;
    end
end

L2_f
```

A.4 Example MATLAB code for stepwise regression and sensitivity analysis

```
clc
tic

load('H2_L_DA.mat','H2_L_DA');
```

```
Sample = H2_L_DA';

start = 131;
holder =  start - 1;
last = 268;

Means = mean(Sample);

for counter4 = start:last
    [plot_purpose,~,pval] = stepwisefit(Sample,P_TUSE3(counter4,:)');
    pval_storage(:,counter4-holder) = pval;
    plot_purpose2(:,counter4-holder) = plot_purpose
end

%%
figure
subplot(1,2,1)
for counter3 = start:last
    for counter4 = 1:32
        if pval_storage(counter4,counter3-holder)<=0.05
            scatter(xm(counter3)*1000,counter4,'.')
            hold on
        end
    end
    ylim([0 40])
end
ylabel('Reaction Number')
xlabel('Distance in mm from inlet')
title('Finding most important reactions')
% H2 Loss Plot
subplot(1,2,2)

for counter4 = [3,18,21]
    plot(xm(131:268)*1000,smooth(plot_purpose2(counter4,:),'loess'))
    hold on
end

legend('R3','R18','R21','Location','best')
xlabel('Distance from injectors (mm)')
ylabel('Sensitivity  Coefficients')
title('Sensitivity of different reactions')
```

A.5 Example MATLAB code for Monte Carlo simulation

```
clc

load('H2_L_DA.mat','H2_L_DA');
Sample = H2_L_DA';
start = 131;
last = 268;
```

```
Means = mean(Sample);
rng

%% 1000 points
points = 1000; %remember to change title of the graph

tic
Super_matrix = zeros(points,32);

    for j = 1:32
    Super_matrix(:,j) = randn(points,1)*20.92+Means(j)
    end

Check = mean(Super_matrix)
Check_2 = Check - Means
F = mean(Check_2)
toc

tic
Total2 = zeros(139,points);
for counter2 = 131:268
    plate_model1 =
stepwiselm(Sample,P_TUSE3(counter2,1:33)','constant','Upper','linear','PEnter
',0.05);
    for counter3 = 1:points
        trial2 = predict(plate_model1,Super_matrix(counter3,:));
        Total2(counter2-130,counter3) = sum(trial2);
    end
    counter2
end
toc

Mean_real = mean(Total2,2); STD_real = std(Total2,0,2);
plus_plot = Mean_real+STD_real; minus_plot = Mean_real-STD_real;

%% 5000 points
points = 5000; %remember to change title of the graph

tic
Super_matrix_2 = zeros(points,32);

    for j = 1:32
    Super_matrix_2(:,j) = randn(points,1)*20.92+Means(j)
    end

Check = mean(Super_matrix_2);
Check_2 = Check - Means;
F = mean(Check_2)
toc

tic
Total2 = zeros(139,points);
for counter2 = 131:289
```

```
    plate_model1 =
stepwiselm(Sample,P_TUSE3(counter2,:)','constant','Upper','linear','PEnter',0
.05);
    for counter3 = 1:points
        trial2 = predict(plate_model1,Super_matrix_2(counter3,:));
        Total2(counter2-130,counter3) = sum(trial2);
    end
    counter2
end
toc

Mean_real_2 = mean(Total2,2); STD_real_2 = std(Total2,0,2);
plus_plot_2 = Mean_real_2+STD_real_2; minus_plot_2 = Mean_real_2-STD_real_2;

%% 10000 points
points = 10000; %remember to change title of the graph

tic
Super_matrix_3 = zeros(points,32);

    for j = 1:32
    Super_matrix_3(:,j) = randn(points,1)*20.92+Means(j)
    end

Check = mean(Super_matrix_3);
Check_3 = Check - Means;
F = mean(Check_3)
toc

tic
Total2 = zeros(139,points);
for counter2 = 131:289
    plate_model1 =
stepwiselm(Sample,P_TUSE3(counter2,:)','constant','Upper','linear','PEnter',0
.05);
    for counter3 = 1:points
        trial2 = predict(plate_model1,Super_matrix_3(counter3,:));
        Total2(counter2-130,counter3) = sum(trial2);
    end
    counter2
end
toc

Mean_real_3 = mean(Total2,2); STD_real_3 = std(Total2,0,2);
plus_plot_3 = Mean_real_3+STD_real_3; minus_plot_3 = Mean_real_3-STD_real_3;

Mean_final =  Mean_real-Mean_real_2
STD_final = STD_real-STD_real_2
%%
close all
last  =  268
figure
plot(xm(start:last)*1000,plus_plot(1:138),'b')
hold on
```

```
plot(xm(start:last)*1000,plus_plot_2(1:138),'g')
plot(xm(start:last)*1000,plus_plot_3(1:138),'k')
title('1000 points vs 5000 points vs Baseline for H2 Loss')
plot(xm(start:last)*1000,Mean_real(1:138),'b')
plot(xm(start:last)*1000,Mean_real_2(1:138),'g')
plot(xm(start:last)*1000,Mean_real_3(1:138),'k')
plot(xm(start:last)*1000,minus_plot(1:138),'b')
plot(xm(start:last)*1000,minus_plot_2(1:138),'g')
plot(xm(start:last)*1000,minus_plot_3(1:138),'k')
plot(xm(start:last)*1000,P_TUSE3_baseline(131:268),'r')
legend('1k top','5k top','1k mean','5k mean','1k bottom','5k
bottom','actual','location','best')
xlabel('Distance in mm from inlet')
ylabel('Mass fraction of WSe_3')
```

Appendix B

Sampling set for CO release reactions

	k1	k2	k3	k4	k5	k6	k7	k8	k9	k10	k11	k12	k13	k14	k15	k16	k17	k18	k19	k20	k21	k22	k23	k24	k25	k26	k27	k28	k29	k30	k31	k32	k33	k34	k35	k36	k37	k38	k39	k40	k41	k42	k43	k44	k45	k46
n1	39	1	46	1	16	8	12	8	40	17	27	33	38	20	43	27	7	11	40	41	23	26	38	46	13	9	39	21	34	36	15	11	29	28	41	40	44	20	18	29	15	42	44	28	12	45
n2	14	46	11	20	24	19	40	23	8	1	47	29	1	3	30	37	23	46	42	21	29	1	40	18	22	19	41	23	23	18	5	18	41	24	6	47	25	16	1	12	35	38	19	37	7	11
n3	2	45	1	39	9	21	44	31	28	24	6	20	31	18	37	45	28	3	41	33	42	46	28	34	23	25	4	10	24	15	43	42	46	28	34	23	42	46	28	18	44	33	18	30	37	44
n4	9	9	6	29	26	6	35	28	2	38	40	37	42	22	39	9	5	40	20	25	1	36	30	33	43	43	20	47	28	37	8	27	12	41	47	32	19	41	21	35	42	15	17	33	33	19
n5	26	38	22	15	15	22	27	14	39	30	5	36	40	21	42	24	41	1	29	38	38	3	43	21	39	44	24	13	7	28	3	40	32	22	25	25	34	42	12	34	8	11	16	15	46	1
n6	18	43	45	8	5	2	29	18	3	34	17	38	18	9	23	23	1	33	32	15	24	24	5	15	3	37	25	42	25	23	34	41	9	1	19	33	20	8	23	22	5	4	32	1	39	36
n7	40	7	3	26	35	17	19	2	45	19	18	25	12	16	20	20	8	32	39	24	36	19	22	37	34	3	43	37	19	7	19	36	2	4	9	4	6	38	20	13	38	7	7	38	42	42
n8	44	33	28	24	42	35	39	44	20	27	45	16	39	7	9	42	2	16	1	6	40	17	13	41	47	33	28	3	27	43	27	42	35	10	29	29	37	33	28	7	19	23	34	30	37	40
n9	34	34	27	16	47	42	43	42	27	22	15	41	15	25	6	7	3	12	44	35	6	45	44	12	19	39	29	31	15	31	7	16	30	9	17	8	9	36	40	17	12	46	12	12	10	29
n10	37	25	13	11	8	43	24	26	4	9	7	5	37	36	10	17	17	41	37	30	12	5	15	32	29	6	2	30	22	5	20	22	47	13	38	36	11	25	38	38	21	43	38	27	47	21
n11	28	35	15	3	25	47	33	4	47	42	16	32	19	44	17	38	21	31	4	9	15	29	14	5	45	1	23	46	24	40	22	29	25	36	21	46	28	14	7	41	10	24	6	21	6	32
n12	10	18	25	21	28	23	13	38	23	21	14	9	24	2	35	3	39	36	35	10	42	33	3	28	41	8	9	36	29	27	4	44	27	43	11	2	29	37	9	14	2	39	43	6	3	24
n13	3	29	10	33	18	39	28	43	44	36	39	40	10	26	13	11	25	30	31	32	35	39	33	20	32	7	33	26	16	15	21	7	37	19	46	14	47	3	27	20	34	1	47	10	40	25
n14	22	32	20	37	13	18	22	47	35	14	21	24	9	29	41	18	16	4	6	19	31	4	28	13	14	20	4	45	46	14	36	9	7	20	43	26	42	35	10	2	25	45	2	18	41	39
n15	45	6	30	28	34	28	46	24	6	10	9	27	43	6	33	16	35	13	33	20	37	23	27	10	38	24	1	33	5	21	45	6	19	11	20	27	36	9	11	40	47	9	20	14	1	34
n16	35	28	42	34	22	36	26	12	24	25	34	28	5	31	36	30	47	43	22	31	5	7	42	6	28	25	18	6	35	34	32	47	17	16	45	11	2	45	17	23	40	19	46	4	18	46
n17	25	39	32	23	21	32	3	30	29	31	3	26	36	12	3	43	38	42	34	4	43	47	46	31	24	42	26	28	39	33	26	4	6	39	13	34	8	23	14	30	46	41	33	22	44	33
n18	29	44	36	30	27	30	34	22	38	6	22	14	41	28	46	35	18	45	9	23	47	32	45	34	17	32	21	41	38	1	18	26	34	30	44	7	5	6	45	27	7	2	15	35	2	18
n19	31	2	8	35	3	27	15	36	30	16	13	21	33	15	5	34	43	38	43	18	9	16	17	4	27	45	38	9	26	17	10	20	10	31	37	39	43	19	44	6	3	8	5	23	8	41
n20	20	15	43	19	4	41	47	40	36	12	10	17	7	46	47	4	22	34	27	37	27	34	2	38	40	40	37	7	17	39	38	19	11	26	12	37	7	11	15	3	29	21	22	41	31	13
n21	12	4	12	31	41	12	23	34	31	33	29	10	28	34	25	36	30	2	46	26	39	41	10	3	15	35	31	29	44	19	37	37	44	3	40	45	1	34	4	32	14	26	31	36	24	16
n22	17	47	16	45	17	5	18	7	17	15	19	19	32	45	11	39	14	29	14	44	44	34	37	7	25	25	26	13	10	1	32	11	1	8	6	32	13	27	44	3	19	13	31	36	29	4
n23	23	11	26	44	1	38	11	3	16	8	38	43	8	17	16	15	12	10	17	14	41	11	16	11	37	47	47	34	38	18	29	39	10	39	44	18	9	12	29	36	46	6	34	40	44	25
n24	19	13	7	12	19	20	20	41	34	4	46	11	29	30	21	21	9	21	8	40	44	31	36	2	4	16	8	5	3	26	14	45	3	46	24	28	2	5	15	43	31	29	25	11	29	38
n25	30	30	4	14	7	24	7	1	42	26	44	6	34	19	38	10	11	28	28	8	3	43	39	9	35	41	6	11	40	22	46	24	28	2	5	15	40	22	29	10	27	32	29	25	22	4
n26	41	27	38	36	2	1	10	45	32	11	33	45	20	42	19	28	45	9	11	7	7	42	24	44	30	15	19	40	9	10	13	35	43	14	3	43	17	40	35	18	37	14	28	20	13	20
n27	5	36	35	18	38	10	1	33	43	18	32	15	45	1	22	6	42	27	3	39	8	2	9	17	36	18	45	34	12	41	31	8	26	5	31	22	3	7	34	31	30	37	14	17	28	22
n28	24	40	5	6	39	34	2	27	12	3	8	47	44	41	32	22	20	17	23	13	13	27	6	23	5	30	47	14	13	11	44	43	36	47	35	6	32	21	8	15	44	22	26	19	20	27
n29	13	24	17	5	45	4	31	21	7	37	11	27	38	27	8	36	22	12	16	25	14	47	16	23	14	22	18	20	24	42	2	33	42	10	35	14	39	39	1	1	5	42	42	30	43
n30	7	23	47	43	31	11	42	13	33	32	23	2	26	33	15	2	29	35	21	2	11	28	32	27	11	34	30	12	8	4	17	38	38	21	23	16	45	10	6	45	24	40	11	40	38	47
n31	47	16	2	27	32	7	36	19	37	13	4	8	3	23	2	5	24	18	2	17	18	10	23	42	1	38	27	24	43	45	12	15	31	27	27	23	23	17	16	36	32	10	41	5	16	3
n32	43	19	40	47	30	31	32	39	41	39	36	42	47	10	18	31	13	37	25	42	2	13	12	14	7	12	14	20	33	6	33	12	22	45	1	17	18	32	2	21	11	13	37	34	32	6
n33	6	14	37	41	10	14	30	9	13	23	1	12	25	11	1	33	4	14	13	43	22	35	41	19	44	2	40	16	31	16	43	39	40	40	28	28	21	27	26	5	36	30	3	21	7	7
n34	38	31	23	40	40	25	38	10	19	5	37	18	16	14	31	29	46	25	38	12	16	46	25	29	9	4	32	35	2	44	47	33	4	34	42	31	35	28	41	25	4	35	21	26	45	2
n35	15	21	29	2	33	9	41	15	46	43	26	22	14	24	12	46	30	23	30	29	26	6	8	26	26	46	10	39	4	2	30	31	13	37	39	20	31	26	46	11	45	44	45	31	9	10
n36	32	37	19	46	36	16	14	11	21	44	41	44	30	47	14	1	27	24	47	28	46	8	19	45	33	21	5	8	37	30	29	32	24	35	22	38	15	1	33	16	23	36	3	7	14	23
n37	27	26	34	13	23	15	21	25	26	46	6	8	26	14	26	47	19	27	45	38	4	7	6	10	11	2	36	38	23	23	46	18	34	19	38	46	47	37	43	20	1	47	26	17	26	17
n38	33	41	24	4	11	40	4	35	10	46	35	4	4	4	7	12	32	7	26	47	19	30	34	47	20	28	17	25	14	13	41	30	15	32	36	24	22	31	5	33	16	6	9	45	5	28
n39	46	12	9	17	20	3	25	46	1	41	20	34	13	37	34	40	37	39	7	36	30	25	35	22	42	42	22	46	19	32	12	35	28	14	15	14	1	33	2	22	44	9	47	24	24	14
n40	11	20	44	10	46	13	8	37	25	7	31	13	2	40	28	47	6	19	45	5	10	18	20	30	46	23	12	4	30	20	24	3	21	38	24	12	26	30	47	30	39	26	28	18	13	11
n41	1	17	31	7	12	44	45	16	14	20	43	30	46	35	8	13	40	20	18	11	33	15	21	39	12	13	44	17	47	9	25	14	1	8	16	21	30	47	30	39	26	28	18	13	11	9
n42	21	3	14	9	14	29	37	5	15	29	42	31	23	13	29	44	44	5	10	22	17	44	11	36	10	27	7	15	21	25	6	5	42	29	26	5	4	4	13	4	20	27	4	8	43	37
n43	8	10	21	42	37	45	5	20	18	40	2	39	11	5	44	26	10	15	5	3	14	20	29	35	16	17	15	1	10	8	9	25	5	7	33	44	10	12	31	28	17	33	39	32	15	8
n44	42	42	33	32	43	33	17	6	5	28	28	3	17	27	40	19	31	6	16	45	21	40	1	8	31	29	42	27	45	3	1	13	16	33	8	42	39	24	42	26	39	17	35	16	36	31
n45	36	22	39	25	6	26	16	32	9	47	30	1	35	43	24	25	15	8	36	1	28	9	31	1	8	5	36	32	11	47	2	211	20	23	30	3	16	13	24	8	41	16	23	39	23	5
n46	16	8	18	38	29	46	9	29	22	45	25	7	21	32	45	41	19	44	24	34	32	12	26	43	2	36	35	44	6	35	40	17	45	17	2	30	41	43	32	24	28	25	13	2	19	30
n47	4	5	41	22	44	37	6	17	11	2	24	35	22	39	4	32	34	26	15	46	20	22	37	24	21	31	3	43	41	42	16	46	18	12	15	18	46	5	19	9	22	12	27	46	35	15

Appendix C

Chemical Model

```
#T6-TUC6O6reactions
1: T6-TUC6O6->T5-TUC5O5+CO   {A = 1.20E+16 n = 0.00 E = 154.9246}

#T5reactions
2: T5-TUC5O5->T4-TUC4O4+CO   {A = 1.60E+15 n = 0.00 E = 157.2366}
3f: T5-TUC5O5+S2-H2SE->T5S2-TUC5O5H2SE   {A = 5.28E+12 n = 0.00 E = 0.0000}
3b: T5S2-TUC5O5H2SE->T5-TUC5O5+S2-H2SE   {A = 3.19E+12 n = 0.00 E = 31.0578}
4: T5S2-TUC5O5H2SE->T4S2-TUC4O4H2SE+CO   {A = 2.92E+16 n = 0.00 E = 154.9254}

#T4reactions
5: T4-TUC4O4->T3-TUC3O3+CO   {A = 4.66E+14 n = 0.00 E = 161.2753}
6f: T4-TUC4O4+S2-H2SE->T4S2-TUC4O4H2SE   {A = 5.13E+12 n = 0.00 E = 0.0000}
6b: T4S2-TUC4O4H2SE->T4-TUC4O4+S2-H2SE   {A = 2.12E+12 n = 0.00 E = 27.5658}
7: T4S2-TUC4O4H2SE->T3S2-TUC3O3H2SE+CO   {A = 1.29E+16 n = 0.00 E = 128.6851}
8f: T4S2-TUC4O4H2SE+S2-H2SE->T4GS2G2-TUC4O4H4SE2     {A = 5.53E+12 n = 0.00 E = 0.0000}
8b: T4GS2G2-TUC4O4H4SE2->T4S2-TUC4O4H2SE+S2-H2SE     {A = 4.00E+12 n = 0.00 E = 32.5877}
9: T4GS2G2-TUC4O4H4SE2->T3GS2G2-TUC3O3H4SE2+CO   {A = 2.08E+15 n = 0.00 E = 90.9907}
10f: T4GS2G2-TUC4O4H4SE2->T4GS1G2-TUC4O4H2SE2+H2     {A = 4.57E+13 n = 0.00 E = 55.3432}
10b: T4GS1G2-TUC4O4H2SE2+H2->T4GS2G2-TUC4O4H4SE2     {A = 2.43E+13 n = 0.00 E = 113.3616}
11: T4GS1G2-TUC4O4H2SE2->T3GS1G2-TUC3O3H2SE2+CO  {A = 4.02E+15 n = 0.00 E = 105.0242}
12f: T4GS1G2-TUC4O4H2SE2->T4GSEG2-TUC4O4SE2+H2   {A = 7.40E+13 n = 0.00 E = 59.8576}
12b: T4GSEG2-TUC4O4SE2+H2->T4GS1G2-TUC4O4H2SE2   {A = 2.43E+13 n = 0.00 E = 103.3296}
13: T4GSEG2-TUC4O4SE2->T3SE2-TUC3O3SE2+CO    {A = 4.66E+14 n = 0.00 E = 77.0625}

#T3reactions
14: T3-TUC3O3->T2-TUC2O2+CO  {A = 9.96E+16 n = 0.00 E = 272.1356}
15f: T3-TUC3O3+S2-H2SE->T3S2-TUC3O3H2SE  {A = 4.99E+12 n = 0.00 E = 0.0000}
15b: T3S2-TUC3O3H2SE->T3-TUC3O3+S2-H2SE  {A = 2.01E+14 n = 0.00 E = 70.4142}
16: T3S2-TUC3O3H2SE->T2S2-TUC2O2H2SE+CO  {A = 5.49E+14 n = 0.00 E = 283.4190}
17f: T3S2-TUC3O3H2SE+S2-H2SE->T3GS2G2-TUC3O3H4SE2    {A = 5.40E+12 n = 0.00 E = 0.0000}
17b: T3GS2G2-TUC3O3H4SE2->T3S2-TUC3O3H2SE+S2-H2SE    {A = 4.18E+13 n = 0.00 E = 54.7998}
18: T3GS2G2-TUC3O3H4SE2->T2GS2G2-TUC2O2H4SE2+CO  {A = 1.92E+15 n = 0.00 E = 223.3825}
19f: T3GS2G2-TUC3O3H4SE2+S2-H2SE->T3GS2G3-TUC3O3H6SE3    {A = 5.78E+12 n = 0.00 E = 0.0000}
19b: T3GS2G3-TUC3O3H6SE3->T3GS2G2-TUC3O3H4SE2+S2-H2SE    {A = 5.20E+13 n = 0.00 E = 56.0275}
20: T3GS2G3-TUC3O3H6SE3->T2GS2G3-TUC2O2H6SE3+CO  {A = 1.19E+16 n = 0.00 E = 110.0176}
21f: T3GS2G2-TUC3O3H4SE2->T3GS1G2-TUC3O3H2SE2+H2     {A = 5.76E+12 n = 0.00 E = 36.2928}
21b: T3GS1G2-TUC3O3H2SE2+H2->T3GS2G2-TUC3O3H4SE2     {A = 2.36E+13 n = 0.00 E = 105.0300}
22: T3GS1G2-TUC3O3H2SE2->T2GS1G2-TUC2O2H2SE2+CO  {A = 7.53E+14 n = 0.00 E = 81.8114}
23f: T3GS1G2-TUC3O3H2SE2+S2-H2SE->T3S2S12-TUC3O3H4SE3    {A = 5.77E+12 n = 0.00 E = 0.0000}
23b: T3S2S12-TUC3O3H4SE3->T3GS1G2-TUC3O3H2SE2+S2-H2SE    {A = 3.18E+12 n = 0.00 E = 29.9568}
24: T3S2S12-TUC3O3H4SE3->T2S2S12-TUC2O2H4SE3+CO  {A = 6.85E+13 n = 0.00 E = 58.6232}
25f: T3S2S12-TUC3O3H4SE3->T3S2SE2-TUC3O3H2SE3+H2     {A = 2.43E+12 n = 0.00 E = 27.4563}
25b: T3S2SE2-TUC3O3H2SE3+H2->T3S2S12-TUC3O3H4SE3     {A = 2.56E+13 n = 0.00 E = 43.9318}
26: T3S2SE2-TUC3O3H2SE3->T2S2SE2-TUC2O2H2SE3+CO  {A = 2.28E+15 n = 0.00 E = 100.8216}
27f: T3GS1G2-TUC3O3H2SE2->T3SE2-TUC3O3SE2+H2     {A = 8.54E+13 n = 0.00 E = 61.4949}
27b: T3SE2-TUC3O3SE2+H2->T3GS1G2-TUC3O3H2SE2     {A = 2.35E+13 n = 0.00 E = 69.7224}
28: T3SE2-TUC3O3SE2->T2SE2-TUC2O2SE2+CO  {A = 2.02E+15 n = 0.00 E = 91.0404}
29f: T3SE2-TUC3O3SE2+S2-H2SE->T3S2SE2-TUC3O3H2SE3    {A = 5.76E+12 n = 0.00 E = 0.0000}
29b: T3S2SE2-TUC3O3H2SE3->T3SE2-TUC3O3SE2+S2-H2SE    {A = 4.51E+12 n = 0.00 E = 33.2348}

#T2reactions
30: T2-TUC2O2->T1-TUC1O1+CO  {A = 2.65E+14 n = 0.00 E = 234.3810}
31f: T2-TUC2O2+S2-H2SE->T2S2-TUC2O2H2SE  {A = 4.84E+12 n = 0.00 E = 0.0000}
31b: T2S2-TUC2O2H2SE->T2-TUC2O2+S2-H2SE  {A = 2.72E+14 n = 0.00 E = 73.6533}
32f: T2S2-TUC2O2H2SE+S2-H2SE->T2GS2G2-TUC2O2H4SE2    {A = 5.26E+12 n = 0.00 E = 0.0000}
32b: T2GS2G2-TUC2O2H4SE2->T2S2-TUC2O2H2SE+S2-H2SE    {A = 2.26E+14 n = 0.00 E = 70.8493}
33f: T2GS2G2-TUC2O2H4SE2+S2-H2SE->T2GS2G3-TUC2O2H6SE3    {A = 5.65E+12 n = 0.00 E = 0.0000}
33b: T2GS2G3-TUC2O2H6SE3->T2GS2G2-TUC2O2H4SE2+S2-H2SE    {A = 2.03E+14 n = 0.00 E = 69.0248}
34f: T2GS2G3-TUC2O2H6SE3+S2-H2SE->T2GS2G4-TUC2O2H8SE4    {A = 6.02E+12 n = 0.00 E = 0.0000}
34b: T2GS2G4-TUC2O2H8SE4->T2GS2G3-TUC2O2H6SE3+S2-H2SE    {A = 3.25E+14 n = 0.00 E = 72.6835}
35f: T2GS2G2-TUC2O2H4SE2->T2GS1G2-TUC2O2H2SE2+H2     {A = 2.02E+12 n = 0.00 E = 26.8072}
```

```
35b: T2GS1G2-TUC2O2H2SE2+H2->T2GS2G2-TUC2O2H4SE2     {A = 2.28E+13 n = 0.00 E = 163.1872}
36f: T2GS2G3-TUC2O2H6SE3->T2S2S12-TUC2O2H4SE3+H2     {A = 2.33E+12 n = 0.00 E = 27.2954}
36b: T2S2S12-TUC2O2H4SE3+H2->T2GS2G3-TUC2O2H6SE3     {A = 2.50E+13 n = 0.00 E = 171.7562}
37f: T2GS2G4-TUC2O2H8SE4->T2S22S12-TUC2O2H6SE4+H2    {A = 2.23E+12 n = 0.00 E = 26.1505}
37b: T2S22S12-TUC2O2H6SE4+H2->T2GS2G4-TUC2O2H8SE4    {A = 2.70E+13 n = 0.00 E = 159.2162}
38f: T2GS1G2-TUC2O2H2SE2+S2-H2SE->T2S2S12-TUC2O2H4SE3    {A = 5.64E+12 n = 0.00 E = 0.0000}
38b: T2S2S12-TUC2O2H4SE3->T2GS1G2-TUC2O2H2SE2+S2-H2SE    {A = 1.12E+14 n = 0.00 E = 63.5038}
39f: T2GS1G2-TUC2O2H2SE2->T2SE2-TUC2O2SE2+H2     {A = 4.07E+14 n = 0.00 E = 76.3891}
39b: T2SE2-TUC2O2SE2+H2->T2GS1G2-TUC2O2H2SE2     {A = 2.27E+13 n = 0.00 E = 60.6100}
40f: T2S2S12-TUC2O2H4SE3->T2S2SE2-TUC2O2H2SE3+H2     {A = 1.30E+15 n = 0.00 E = 93.7390}
40b: T2S2SE2-TUC2O2H2SE3+H2->T2S2S12-TUC2O2H4SE3     {A = 2.49E+13 n = 0.00 E = 61.9476}
41f: T2S2S12-TUC2O2H4SE3+S2-H2SE->T2S22S12-TUC2O2H6SE4   {A = 6.01E+12 n = 0.00 E = 0.0000}
41b: T2S22S12-TUC2O2H6SE4->T2S2S12-TUC2O2H4SE3+S2-H2SE   {A = 5.94E+12 n = 0.00 E = 35.3294}
42f: T2S2SE2-TUC2O2H2SE3+S2-H2SE->T2S22SE2-TUC2O2H4SE4   {A = 6.00E+12 n = 0.00 E = 0.0000}
42b: T2S22SE2-TUC2O2H4SE4->T2S2SE2-TUC2O2H2SE3+S2-H2SE   {A = 8.01E+11 n = 0.00 E = 16.6364}
43f: T2SE2-TUC2O2SE2+S2-H2SE->T2S2SE2-TUC2O2H2SE3    {A = 5.63E+12 n = 0.00 E = 0.0000}
43b: T2S2SE2-TUC2O2H2SE3->T2SE2-TUC2O2SE2+S2-H2SE    {A = 3.48E+12 n = 0.00 E = 31.0933}
44f: T2S22S12-TUC2O2H6SE4->T2GS1G4-TUC2O2H4SE4+H2    {A = 3.59E+14 n = 0.00 E = 73.6165}
44b: T2GS1G4-TUC2O2H4SE4+H2->T2S22S12-TUC2O2H6SE4    {A = 2.70E+13 n = 0.00 E = 154.7854}
45f: T2GS1G4-TUC2O2H4SE4->T2S12SE2-TUC2O2H2SE4+H2    {A = 3.42E+15 n = 0.00 E = 101.6576}
45b: T2S12SE2-TUC2O2H2SE4+H2->T2GS1G4-TUC2O2H4SE4    {A = 2.69E+13 n = 0.00 E = 54.2146}
46f: T2S22SE2-TUC2O2H4SE4->T2S12SE2-TUC2O2H2SE4+H2   {A = 1.04E+15 n = 0.00 E = 83.6000}
46b: T2S12SE2-TUC2O2H2SE4+H2->T2S22SE2-TUC2O2H4SE4   {A = 2.69E+13 n = 0.00 E = 69.3462}
47: T2S2-TUC2O2H2SE->T1S2-TUCOH2SE+CO    {A = 1.26E+18 n = 0.00 E = 259.9454}
48: T2GS2G2-TUC2O2H4SE2->T1GS2G2-TUCOH4SE2+CO    {A = 6.15E+14 n = 0.00 E = 287.7754}
49: T2GS2G3-TUC2O2H6SE3->T1GS2G3-TUCOH6SE3+CO    {A = 1.25E+16 n = 0.00 E = 233.1558}
50: T2GS2G4-TUC2O2H8SE4->T1GS2G4-TUCOH8SE4+CO    {A = 5.85E+16 n = 0.00 E = 232.6881}
51: T2GS1G2-TUC2O2H2SE2->T1GS1G2-TUCOH2SE2+CO    {A = 3.51E+13 n = 0.00 E = 222.1290}
52: T2S2S12-TUC2O2H4SE3->T1S2S12-TUCOH4SE3+CO    {A = 3.45E+15 n = 0.00 E = 256.6553}
53: T2SE2-TUC2O2SE2->T1SE2-TUCOSE2+CO    {A = 1.43E+17 n = 0.00 E = 137.7954}
54: T2S22S12-TUC2O2H6SE4->T1S22S12-TUCOH6SE4+CO  {A = 2.33E+16 n = 0.00 E = 146.8852}
55: T2S2SE2-TUC2O2H2SE3->T1S2SE2-TUCOH2SE3+CO    {A = 1.84E+15 n = 0.00 E = 89.6255}
56: T2GS1G4-TUC2O2H4SE4->T1GS1G4-TUCOH4SE4+CO    {A = 3.95E+15 n = 0.00 E = 260.5269}
57: T2S12SE2-TUC2O2H2SE4->T1S12SE2-TUCOH2SE4+CO  {A = 2.74E+14 n = 0.00 E = 71.1436}

#T1reactions
58f: T1-TUC1O1+S2-H2SE->T1S2-TUCOH2SE    {A = 4.69E+12 n = 0.00 E = 0.0000}
58b: T1S2-TUCOH2SE->T1-TUC1O1+S2-H2SE    {A = 9.10E+14 n = 0.00 E = 87.8636}
59f: T1S2-TUCOH2SE+S2-H2SE->T1GS2G2-TUCOH4SE2    {A = 5.12E+12 n = 0.00 E = 0.0000}
59b: T1GS2G2-TUCOH4SE2->T1S2-TUCOH2SE+S2-H2SE    {A = 3.89E+14 n = 0.00 E = 76.2674}
60f: T1GS2G2-TUCOH4SE2+S2-H2SE->T1GS2G3-TUCOH6SE3    {A = 5.52E+12 n = 0.00 E = 0.0000}
60b: T1GS2G3-TUCOH6SE3->T1GS2G2-TUCOH4SE2+S2-H2SE    {A = 5.61E+14 n = 0.00 E = 78.7846}
61f: T1GS2G3-TUCOH6SE3+S2-H2SE->T1GS2G4-TUCOH8SE4    {A = 5.89E+12 n = 0.00 E = 0.0000}
61b: T1GS2G4-TUCOH8SE4->T1GS2G3-TUCOH6SE3+S2-H2SE    {A = 2.38E+14 n = 0.00 E = 69.9941}
62f: T1GS2G2-TUCOH4SE2->T1GS1G2-TUCOH2SE2+H2     {A = 4.71E+11 n = 0.00 E = 13.5691}
62b: T1GS1G2-TUCOH2SE2+H2->T1GS2G2-TUCOH4SE2     {A = 2.20E+13 n = 0.00 E = 73.6934}
63f: T1GS1G2-TUCOH2SE2->T1SE2-TUCOSE2+H2     {A = 8.59E+12 n = 0.00 E = 40.6977}
63b: T1SE2-TUCOSE2+H2->T1GS1G2-TUCOH2SE2     {A = 2.19E+13 n = 0.00 E = 109.5160}
64f: T1GS2G3-TUCOH6SE3->T1S2S12-TUCOH4SE3+H2     {A = 1.13E+12 n = 0.00 E = 20.8080}
64b: T1S2S12-TUCOH4SE3+H2->T1GS2G3-TUCOH6SE3     {A = 2.42E+13 n = 0.00 E = 127.1138}
65f: T1S2S12-TUCOH4SE3->T1S2SE2-TUCOH2SE3+H2     {A = 1.06E+13 n = 0.00 E = 41.7448}
65b: T1S2SE2-TUCOH2SE3+H2->T1S2S12-TUCOH4SE3     {A = 2.42E+13 n = 0.00 E = 87.7800}
66f: T1GS2G4-TUCOH8SE4->T1S22S12-TUCOH6SE4+H2    {A = 1.90E+12 n = 0.00 E = 24.8865}
66b: T1S22S12-TUCOH6SE4+H2->T1GS2G4-TUCOH8SE4    {A = 2.63E+13 n = 0.00 E = 98.3972}
67f: T1S22S12-TUCOH6SE4->T1S22SE2-TUCOH4SE4+H2   {A = 7.66E+14 n = 0.00 E = 80.9361}
67b: T1S22SE2-TUCOH4SE4+H2->T1S22S12-TUCOH6SE4   {A = 2.63E+13 n = 0.00 E = 115.0336}
68f: T1S22S12-TUCOH6SE4->T1GS1G4-TUCOH4SE4+H2    {A = 1.81E+12 n = 0.00 E = 24.4643}
68b: T1GS1G4-TUCOH4SE4+H2->T1S22S12-TUCOH6SE4    {A = 2.63E+13 n = 0.00 E = 141.7438}
69f: T1S22SE2-TUCOH4SE4->T1S12SE2-TUCOH2SE4+H2   {A = 2.83E+13 n = 0.00 E = 50.1512}
69b: T1S12SE2-TUCOH2SE4+H2->T1S22SE2-TUCOH4SE4   {A = 2.62E+13 n = 0.00 E = 98.5644}
70f: T1GS1G4-TUCOH4SE4->T1S12SE2-TUCOH2SE4+H2    {A = 2.19E+12 n = 0.00 E = 26.2592}
70b: T1S12SE2-TUCOH2SE4+H2->T1GS1G4-TUCOH4SE4    {A = 2.62E+13 n = 0.00 E = 78.9602}
71f: T1GS1G2-TUCOH2SE2+S2-H2SE->T1S2S12-TUCOH4SE3    {A = 5.51E+12 n = 0.00 E = 0.0000}
71b: T1S2S12-TUCOH4SE3->T1GS1G2-TUCOH2SE2+S2-H2SE    {A = 1.50E+14 n = 0.00 E = 66.4758}
72f: T1SE2-TUCOSE2+S2-H2SE->T1S2SE2-TUCOH2SE3    {A = 5.50E+12 n = 0.00 E = 0.0000}
72b: T1S2SE2-TUCOH2SE3->T1SE2-TUCOSE2+S2-H2SE    {A = 8.22E+13 n = 0.00 E = 60.8980}
73f: T1S2S12-TUCOH4SE3+S2-H2SE->T1S22S12-TUCOH6SE4   {A = 5.88E+12 n = 0.00 E = 0.0000}
73b: T1S22S12-TUCOH6SE4->T1S2S12-TUCOH4SE3+S2-H2SE   {A = 2.92E+15 n = 0.00 E = 99.9902}
```

```
74f: T1S2SE2-TUCOH2SE3+S2-H2SE->T1S22SE2-TUCOH4SE4   {A = 5.87E+12 n = 0.00 E = 0.0000}
74b: T1S22SE2-TUCOH4SE4->T1S2SE2-TUCOH2SE3+S2-H2SE   {A = 2.28E+14 n = 0.00 E = 69.6229}
75: T1S2-TUCOH2SE->TUS2-TUH2SE+CO    {A = 2.03E+16 n = 0.00 E = 271.4877}
76: T1GS2G2-TUCOH4SE2->TUGS2G2-TUH4SE2+CO    {A = 4.69E+13 n = 0.00 E = 262.8208}
77: T1GS2G3-TUCOH6SE3->TUGS2G3-TUH6SE3+CO    {A = 2.91E+15 n = 0.00 E = 247.1906}
78: T1GS2G4-TUCOH8SE4->TUGS2G4-TUH8SE4+CO    {A = 1.60E+16 n = 0.00 E = 242.7552}
79: T1GS1G2-TUCOH2SE2->TUGS1G2-TUH2SE2+CO    {A = 5.90E+16 n = 0.00 E = 241.6638}
80: T1SE2-TUCOSE2->TUSE2+CO  {A = 5.21E+14 n = 0.00 E = 275.5452}
81: T1S2S12-TUCOH4SE3->TUS2S12-TUH4SE3+CO    {A = 6.03E+14 n = 0.00 E = 280.0717}
82: T1S2SE2-TUCOH2SE3->TUS2SE2-TUH2SE3+CO    {A = 1.76E+18 n = 0.00 E = 265.6658}
83: T1S22S12-TUCOH6SE4->TUS22S12-TUH6SE4+CO  {A = 5.94E+15 n = 0.00 E = 291.4028}
84: T1S22SE2-TUCOH4SE4->TUS22SE2-TUH4SE4+CO  {A = 3.28E+14 n = 0.00 E = 220.4653}
85: T1S12SE2-TUCOH2SE4->TUS12SE2-TUH2SE4+CO  {A = 9.84E+14 n = 0.00 E = 182.2480}
86: T1GS1G4-TUCOH4SE4->TUGS1G4-TUH4SE4+CO    {A = 6.64E+14 n = 0.00 E = 281.5138}

#TUreactions
87f: TUS2-TUH2SE+S2-H2SE->TUGS2G2-TUH4SE2    {A = 4.98E+12 n = 0.00 E = 0.0000}
87b: TUGS2G2-TUH4SE2->TUS2-TUH2SE+S2-H2SE    {A = 2.09E+15 n = 0.00 E = 93.1442}
88f: TUGS2G2-TUH4SE2+S2-H2SE->TUGS2G3-TUH6SE3    {A = 5.38E+12 n = 0.00 E = 0.0000}
88b: TUGS2G3-TUH6SE3->TUGS2G2-TUH4SE2+S2-H2SE    {A = 4.25E+14 n = 0.00 E = 76.4940}
89f: TUGS2G3-TUH6SE3+S2-H2SE->TUGS2G4-TUH8SE4    {A = 5.77E+12 n = 0.00 E = 0.0000}
89b: TUGS2G4-TUH8SE4->TUGS2G3-TUH6SE3+S2-H2SE    {A = 2.83E+12 n = 0.00 E = 28.8838}
90f: TUGS2G2-TUH4SE2->TUGS1G2-TUH2SE2+H2     {A = 1.30E+12 n = 0.00 E = 23.4218}
90b: TUGS1G2-TUH2SE2+H2->TUGS2G2-TUH4SE2     {A = 2.11E+13 n = 0.00 E = 191.9038}
91f: TUGS1G2-TUH2SE2->TUSE2+H2   {A = 1.36E+13 n = 0.00 E = 45.9825}
91b: TUSE2+H2->TUGS1G2-TUH2SE2   {A = 2.11E+13 n = 0.00 E = 104.8762}
92f: TUGS1G2-TUH2SE2+S2-H2SE->TUS2S12-TUH4SE3    {A = 5.37E+12 n = 0.00 E = 0.0000}
92b: TUS2S12-TUH4SE3->TUGS1G2-TUH2SE2+S2-H2SE    {A = 8.38E+13 n = 0.00 E = 61.3461}
93f: TUGS2G3-TUH6SE3->TUS2S12-TUH4SE3+H2     {A = 1.02E+12 n = 0.00 E = 20.1447}
93b: TUS2S12-TUH4SE3+H2->TUGS2G3-TUH6SE3     {A = 2.35E+13 n = 0.00 E = 184.0454}
94f: TUS2S12-TUH4SE3->TUS2SE2-TUH2SE3+H2     {A = 3.00E+13 n = 0.00 E = 51.7622}
94b: TUS2SE2-TUH2SE3+H2->TUS2S12-TUH4SE3     {A = 2.34E+13 n = 0.00 E = 109.1398}
95f: TUS2SE2-TUH2SE3+S2-H2SE->TUS22SE2-TUH4SE4   {A = 5.75E+12 n = 0.00 E = 0.0000}
95b: TUS22SE2-TUH4SE4->TUS2SE2-TUH2SE3+S2-H2SE   {A = 1.54E+14 n = 0.00 E = 66.2459}
96f: TUS2S12-TUH4SE3+S2-H2SE->TUS22S12-TUH6SE4   {A = 5.76E+12 n = 0.00 E = 0.0000}
96b: TUS22S12-TUH6SE4->TUS2S12-TUH4SE3+S2-H2SE   {A = 6.77E+13 n = 0.00 E = 58.5430}
97f: TUGS2G4-TUH8SE4->TUS22S12-TUH6SE4+H2    {A = 9.76E+11 n = 0.00 E = 18.9371}
97b: TUS22S12-TUH6SE4+H2->TUGS2G4-TUH8SE4    {A = 2.56E+13 n = 0.00 E = 189.2286}
98f: TUS22S12-TUH6SE4->TUS22SE2-TUH4SE4+H2   {A = 2.21E+12 n = 0.00 E = 26.5685}
98b: TUS22SE2-TUH4SE4+H2->TUS22S12-TUH6SE4   {A = 2.56E+13 n = 0.00 E = 113.1526}
99f: TUS22S12-TUH6SE4->TUGS1G4-TUH4SE4+H2    {A = 2.00E+11 n = 0.00 E = 4.1637}
99b: TUGS1G4-TUH4SE4+H2->TUS22S12-TUH6SE4    {A = 2.56E+13 n = 0.00 E = 189.8974}
100f: TUS22SE2-TUH4SE4->TUS12SE2-TUH2SE4+H2  {A = 3.05E+11 n = 0.00 E = 8.1280}
100b: TUS12SE2-TUH2SE4+H2->TUS22SE2-TUH4SE4  {A = 2.55E+13 n = 0.00 E = 199.0098}
101f: TUGS1G4-TUH4SE4->TUS12SE2-TUH2SE4+H2   {A = 7.09E+13 n = 0.00 E = 58.9911}
101b: TUS12SE2-TUH2SE4+H2->TUGS1G4-TUH4SE4   {A = 2.55E+13 n = 0.00 E = 57.6840}

#NEW reactions added after August
102f: T3GS2G3-TUC3O3H6SE3->T3S2S12-TUC3O3H4SE3+H2    {A = 4.14E+16 n = 0.00 E = 124.1460}
102b: T3S2S12-TUC3O3H4SE3+H2->T3GS2G3-TUC3O3H6SE3    {A = 2.57E+13 n = 0.00 E = 61.0280}
103: T1-TUC1O1->TU+CO    {A = 8.30E+12 n = 0.00 E = 121.6380}
104f: TU+S2-H2SE->TUS2-TUH2SE    {A = 2.41E+13 n = 0.00 E = 0.0000}
104b: TUS2-TUH2SE->TU+S2-H2SE    {A = 7.03E+13 n = 0.00 E = 79.8380}
105f: TUSE3+S2-H2SE->TUS12SE2-TUH2SE4    {A = 3.34E+13 n = 0.00 E = 0.0000}
105b: TUS12SE2-TUH2SE4->TUSE3+S2-H2SE    {A = 3.14E+13 n = 0.00 E = 51.4140}
```

BIBLIOGRAPHY

1. Alsema, E. A., & Nieuwlaar, E. (2000). Energy viability of photovoltaic systems. Energy policy, 28(14), 999-1010.
2. Atkins, P., & De Paula, J. (2013). Elements of physical chemistry. Oxford University Press, USA.
3. Cohen, A. J., Mori-Sánchez, P., & Yang, W. (2008). Insights into current limitations of density functional theory. Science, 321(5890), 792-794.
4. Döll, P., Trautmann, T., Gerten, D., Schmied, H. M., Ostberg, S., Saaed, F., & Schleussner, C. F. (2018). Risks for the global freshwater system at 1.5 C and 2 C global warming. Environmental Research Letters, 13(4), 044038.
5. Döpking, S., & Matera, S. (2017). Error propagation in first-principles kinetic Monte Carlo simulation. Chemical Physics Letters, 674, 28-32.
6. Eichfeld, S. M., Hossain, L., Lin, Y. C., Piasecki, A. F., Kupp, B., Birdwell, A. G., ... & Azcatl, A. (2015). Highly scalable, atomically thin WSe2 grown via metal–organic chemical vapor deposition. ACS nano, 9(2), 2080-2087.
7. Energy Information Administration (2018, July 13). Renewable Energy Explained. Retrieved February 27, 2019, from https://www.eia.gov/energyexplained/?page=renewable_home
8. Energy Information Administration (2019, January 24). Annual Energy Outlook 2019 with projections to 2050 Retrieved October 27, 2019, from https://www.eia.gov/outlooks/aeo/pdf/aeo2019.pdf
9. F. Xia, T. Mueller, et al.., Photocurrent imaging and efficient photon detection in a graphene transistor, Nano Lett. 9 (2009) 1039–1044.
10. Fish, D. J., & Burton, M. R. (1997). The effect of uncertainties in kinetic and photochemical data on model predictions of stratospheric ozone depletion. Journal of Geophysical Research: Atmospheres, 102(D21), 25537-25542.
11. Hernandez, A. S. (2008). Breaking barriers to design dimensions in nearly orthogonal Latin hypercubes. NAVAL POSTGRADUATE SCHOOL MONTEREY CA.
12. Huang, J. K., Pu, J., Hsu, C. L., Chiu, M. H., Juang, Z. Y., Chang, Y. H., ... & Li, L. J. (2013). Large-area synthesis of highly crystalline WSe2 monolayers and device applications. ACS nano, 8(1), 923-930.
13. Jain. A, (2018, May 13). Email.
14. Khrapach, F. Withers, T.H. Bointon, et al.., Novel highly conductive and transparent graphene-based conductors, Adv. Mater. 24 (2012) 2844–2849.
15. Landau, D. P., & Binder, K. (2014). A guide to Monte Carlo simulations in statistical physics. Cambridge university press.
16. McKay, M. D., Beckman, R. J., & Conover, W. J. (1979). Comparison of three methods for selecting values of input variables in the analysis of output from a computer code. Technometrics, 21(2), 239-245.

17. Ostadhossein, A., Rahnamoun, A., Wang, Y., Zhao, P., Zhang, S., Crespi, V. H., & van Duin, A. C. (2017). ReaxFF reactive force-field study of molybdenum disulfide (MoS2). The journal of physical chemistry letters, 8(3), 631-640.
18. R.R. Nair, P. Blake, et al.., Fine structure constant defines visual transparency of graphene, Science 320 (2008) 1156965.
19. S. Bae, H.K. Kim, et al.., 30 in roll-based production of high-quality graphene films for flexible transparent electrodes, Nat. Nanotechnol. 5 (2010) 574–578.
20. Savard, B., Xuan, Y., Bobbitt, B., & Blanquart, G. (2015). A computationally-efficient, semi-implicit, iterative method for the time-integration of reacting flows with stiff chemistry. Journal of Computational Physics, 295, 740-769.
21. Sholl, D., & Steckel, J. A. (2011). Density functional theory: a practical introduction. John Wiley & Sons.
22. Tainter, J. A. (2011). Energy, complexity, and sustainability: A historical perspective. Environmental Innovation and Societal Transitions, 1(1), 89-95.
23. United Nations, Department of Economic and Social Affairs, Population Division (2017). World Population Prospects: The 2017 Revision, Key Findings and Advance Tables. Working Paper No. ESA/P/WP/248.
24. Wiener, N. (1938). The homogeneous chaos. American Journal of Mathematics, 60(4), 897-936.
25. Xuan, Y., Jain, A., Zafar, S., Lotfi, R., Nayir, N., Wang, Y., ... & Redwing, J. M. (2019). Multi-scale modeling of gas-phase reactions in metal-organic chemical vapor deposition growth of WSe2. Journal of Crystal Growth, 527, 125247.
26. Xuan. Y, (2018, May 13). Email.
27. Zhang, K., & Jiang, X. (2018). An investigation of fuel variability effect on bio-syngas combustion using uncertainty quantification. Fuel, 220, 283-295.
28. Zhang, X., Al Balushi, Z. Y., Zhang, F., Choudhury, T. H., Eichfeld, S. M., Alem, N., ... & Redwing, J. M. (2016). Influence of carbon in metalorganic chemical vapor deposition of few-layer WSe 2 thin films. Journal of Electronic Materials, 45(12), 6273-6279.

ACADEMIC VITA

Kartik Khosa

Education

The Pennsylvania State University Schreyer Honors College — Graduating: December 2019
Honors in Bachelor of Science, Mechanical Engineering

Work Experience

Product Engineering Intern, *Cummins Inc,* Columbus, IN, USA (Summer 19)

- Led a team of offshore engineers in designing and simulating a fixture used for thermocycle fatigue test.
- Improved analysis and data visualization efficiency by 60% by leveraging MATLAB GUI.
- Used multivariate regression and hypothesis testing in Minitab to identify and implement improvements in the manufacturing process to meet customer requirements.
- Proposed future fatigue tests for a new design idea that would save $450,000 annually.
- Modified CAD parts in CREO and released them into the system while creating 2D drawings.

Research Assistant, *Computational Reacting Flows Laboratory PSU* (Summer 18-Present)

- Developed a code in MATLAB that automated key input files to eliminate chances of errors during manual data entry and increase efficiency for all stakeholders working on different parts of the project.
- Performed a sensitivity analysis to understand a new cutting-edge manufacturing process: chemical vapor deposition of a new 2-dimensional material.
- Implemented 5 different nearly orthogonal saturated Latin Hypercube sampling designs to reduce cost of simulation by 80-90% and used a Gaussian process as a machine learning technique to make predictive models.

Strategy Intern, *Tech Mahindra Limited,* Shanghai, China (Summer 17)

- Researched local Chinese electric vehicle start-ups for collaboration to improve their existing technology and supply chain as a new revenue stream.
- Created effective meeting agendas that helped capture appropriate client information, needs, concerns while representing the company and then effectively communicated this information to my supervisors.

Projects and Leadership

Liquid-cooled heat sink *(*Fall 18)

- Designed several variations of a heat-sink on SolidWorks for an overheating power system.
- Optimized heat sink designs to reduce power consumption by 5% and reduce heating issues on ANSYS.

PwC Fiercest Competitor Workshop (Fall 18)

- Won the competition to devise a strategy to disrupt the consulting industry and bring PwC's business down.
- Pitched the idea of having Amazon start its own consulting business.

Project Manager, *ME340 Design Methodology Project* (Fall 18)

- Designed a puzzle box that would be used in an escape room at Penn State Mechanical Engineering Department to promote education in STEM in high school students.
- Scheduled an 8-week plan and lead group meetings on regular basis to give guidance and feedback.
- Manufactured 3 prototypes using CNCs, additive manufacturing and machining tools as a team.

Skills and Hobbies

Languages: English, Hindi (Native), Kashmiri (Native), Mandarin (conversational)
Programs: Abaqus, ANSYS, C++(basic), SolidWorks, MS Office, AutoCAD, CREO, MATLAB, Minitab